



Review

Microphysiological systems for recapitulating physiology and function of blood-brain barrier



Suyeong Seo^{a,b}, Hwieun Kim^{a,c}, Jong Hwan Sung^c, Nakwon Choi^{a,d,e}, Kangwon Lee^{b,**},
Hong Nam Kim^{a,d,*}

^a Center for BioMicrosystems, Brain Science Institute, Korea Institute of Science and Technology (KIST), Seoul, 02792, Republic of Korea

^b Program in Nano Science and Technology, Graduate School of Convergence Science and Technology, Seoul National University, Seoul, 08826, Republic of Korea

^c Department of Chemical Engineering, Hongik University, Seoul, 04066, Republic of Korea

^d Division of Bio-Medical Science & Technology, KIST School, Korea University of Science and Technology, Seoul, 02792, Republic of Korea

^e KU-KIST Graduate School of Converging Science and Technology, Korea University, Seoul, 02841, Republic of Korea

ARTICLE INFO

Keywords:

Blood–brain barrier
Neurovascular unit
In vitro models
Physiological relevance
Vascular permeability
Drug screening

ABSTRACT

Central nervous system (CNS) diseases are emerging as a major issue in an aging society. Although extensive research has focused on the development of CNS drugs, the limited transport of therapeutic agents across the blood–brain barrier (BBB) remains a major challenge. Conventional two-dimensional culture dishes do not recapitulate *in vivo* physiology and real-time observations of molecular transport are not possible in animal models. Recent advances in engineering techniques have enabled the generation of more physiologically relevant *in vitro* BBB models, and their applications have expanded from fundamental biological research to practical applications in the pharmaceutical industry. In this article, we provide an overview of recent advances in the development of *in vitro* BBB models, with a particular focus on the recapitulation of BBB function. The development of biomimetic BBB models is postulated to revolutionize not only fundamental biological studies but also drug screening.

1. Introduction

Central nervous system (CNS) diseases are an inevitable issue in an aging society [1]. Despite advances in our understanding of CNS disorders, including Alzheimer's disease, vascular dementia, stroke, and neuronal/vascular malfunctions, the development of therapeutic strategies remains challenging owing to the poor penetration of therapeutic agents through the blood–brain barrier (BBB) [2,3]. As a unique characteristic of the brain, the BBB controls the transport of molecules, such as oxygen, nutrients, drugs, and potentially cytotoxic exogenous substances, between the blood and neural tissues. As a result, substances pass through brain blood vessels *via* limited pathways, including passive diffusion and receptor/carrier-mediated transcytosis [4,5]. If brain tissues are damaged by external injury or disease-associated degeneration, tight junctions (TJs) are disrupted or degraded. Subsequently, the transport mechanism is impaired, allowing macromolecules to uncontrollably enter the neural tissue. This BBB breakdown can cause a homeostatic imbalance and damage to the brain, leading to death [6].

In brain tissues, neurons and glial cells account for 75–90% of the total brain volume, and little space is available for the extracellular matrix (ECM) [7]. Due to the high cell density, approximately 100 billion neurons and glial cells are located 10–20 μ m from blood vessels in the brain [8]. In addition to functions in oxygen and nutrition transport, blood vessels, neurons, astrocytes, and other glial cells communicate *via* direct contact and cytokine-mediated interactions for the survival, growth, and maintenance of brain functions [9,10]. In subjects with neurodegenerative diseases, including Alzheimer's disease, Parkinson's disease, and traumatic brain injury, the anatomy of the BBB is typically disrupted, implying a relationship between CNS diseases and BBB damage [6,11,12]. In the pharmaceutical industry, the barrier function of the BBB limits the delivery of drugs [2,13].

Genetically engineered animal models and *in vitro* models have been developed in response to the growing demand for platforms to study BBB physiology and for drug transport assays. Although animal models benefit from their high similarities to human physiology, they have several limitations, such as the limited availability of real-time imaging,

* Corresponding author. Center for BioMicrosystems, Brain Science Institute, Korea Institute of Science and Technology (KIST), Seoul, 02792, Republic of Korea.

** Corresponding author. Program in Nano Science and Technology, Graduate School of Convergence Science and Technology, Seoul National University, Seoul, 08826, Republic of Korea

E-mail addresses: kangwonlee@snu.ac.kr (K. Lee), hongnam.kim@kist.re.kr (H.N. Kim).

<https://doi.org/10.1016/j.biomaterials.2019.119732>

Received 25 January 2019; Received in revised form 20 December 2019; Accepted 25 December 2019

Available online 26 December 2019

0142-9612/© 2019 Elsevier Ltd. All rights reserved.

time-consuming and cost-ineffective construction, genetic heterogeneity, and ethical issues [14–16]. This different genetic information can lead to unreliable results in drug screening or pathological studies, explaining the failures of pre-clinical screening of thalidomide and Opren. Additionally, in animal models, it is impossible to decouple the independent roles of the ECM and individual cells and to control the biomechanics of brain tissues. *In vitro* models, such as Transwell systems, address some of these limitations [17–20]. These two-dimensional environment-based *in vitro* platforms facilitate the simple and reproducible testing of drug transport in a high-throughput manner, but still have limitations in terms of recapitulating physiological cues, such as cell–cell interactions, cell–matrix interactions, and fluidic shear stress [21]. The importance of microenvironmental factors, including matrix stiffness, fluidic shear stress, blood viscosity, and cellular interactions, in physiological/pathological studies has prompted the development of improved 3D cell culture platforms. Recently developed platforms, including the multilayered microfluidic chip, spheroid-based approach, and hydrogel-laden microfluidic chip, attempt to mimic the important microenvironmental properties of the BBB using engineering techniques [17].

In this review, we provide an overview of recent advances in the development of *in vitro* BBB models. We first summarize the physiologically important aspects of the BBB in terms of its structure, cell–cell and cell–matrix interactions, and microenvironmental cues that support its functions. We also describe recent advances in model development, including conventional Transwell models, multilayered microfluidic models, spheroid-based models, and 3D hydrogel-laden microfluidic models, with a particular focus on how these platforms reflect physiological factors. Finally, we propose future directions for BBB models as a robust tool for fundamental biomedical studies, high-throughput drug screening, and personalized medicine.

2. Physiology of the BBB as a molecular transport barrier

2.1. Comparison of the structure of the BBB and the microvasculature of other organs

The BBB is characterized by its unique structure and cellular composition [22]. Endothelial cells in organs other than the brain have some fenestrae on their membranes, whereas cerebral endothelial cells exhibit low motility and no pores on the cell body [23,24]. Furthermore, cerebral endothelial cells express junctional proteins at higher levels than those in endothelial cells in other organs [25]. In contrast to the typical microvasculature in various human organs, such as the kidney, spleen, lung, and intestines, the BBB is composed of multiple cell types, including brain endothelial cells, astrocytes, and pericytes (Fig. 1) [26]. Interactions among endothelial cells, astrocytes, and pericytes facilitate the formation and maturation of TJs. As a result of (i) the unique lack of fenestrae in cerebral endothelial cells, (ii) the high expression of TJ proteins in cerebral endothelial cells, and (iii) intercellular interactions among the cerebral endothelial cells, astrocytes, and pericytes, the BBB has the distinct ability to limit the transport of molecules by trans-/paracellular diffusion [27–31]. The BBB does not simply prevent the transport of molecules across the endothelium; rather, it selectively transports molecules depending on their sizes and surface characteristics [32,33]. For example, the BBB allows the transport of water and gases, such as oxygen, by passive diffusion, and selectively transports metabolically important substances, such as glucose and amino acids, across the blood and brain interface and TJs (occludin, claudin-5, and zonula occludens) via specific transporters (GLUT-1). Efflux pumps inhibit the penetration of toxins and pathogens through the BBB, maintaining the homeostasis of brain tissues [1,6].

2.2. Tight and adherens junctions

TJs contribute to the regulation of molecular transport

characteristics and are crucial determinants of the specific functions of the BBB. Among various molecular transport pathways, such as paracellular transport, transcellular transport, transcytosis, and pumping, the BBB strictly limits paracellular transport, and this barrier function is mainly attributed to TJs between adjacent cerebral endothelial cells [34,35]. TJs are composed of (i) transmembrane proteins, such as occludin, claudins, and junctional adhesion molecules (JAMs), as the backbone and (ii) peripheral proteins, including zonula occludens (ZO-1, ZO-2, and ZO-3) and the actin cytoskeleton [1,36,37] (Fig. 2a). Transmembrane proteins, the dominant component of TJs, interact with peripheral proteins that are tethered to actin filaments [38–40].

Occludin (65 kDa) is historically the first identified TJ-specific membrane protein [36,37]. Two isoforms of occludin have been identified; however, no differences in their structures and functions have been noted [39]. For the last few decades, transendothelial electrical resistance (TEER) has been used as an indicator of the degree of tightness in the BBB. According to a previous study, electrical resistance across the BBB increases in the presence of occludin [42]. When occludin is degraded by viruses or bacteria, the permeability of brain microvascular endothelial cells increases [36,43]. However, occludin-deficient embryonic stem cells are well differentiated into epithelial cells without any vascular dysfunction, indicating that occludin may not be essential for TJ formation [39]. Claudins, another major element of TJs, are small transmembrane proteins with a molecular weight of 20–27 kDa. Claudin-3, -5, and -12 are prominently expressed in the brain and have fundamental roles in cerebral angiogenesis [37]. Claudin-5- and -12-deficient mouse models display increased vascular permeability to small molecules (< 800 Da) and a disruption of junctional integrity, indicating the importance of Claudins in the formation and function of TJs [44,45]. JAMs (40 kDa), particularly JAM-A, are involved in recruiting and assembling TJ components and maintaining their stability [36,37]. The blockade of JAMs inhibits the reformation of TJs based on a temporary calcium depletion assay, and cold injury decreases JAM-A expression [46,47]. Zonula occludens (ZOs), members of the membrane-associated guanylate kinase (MAGUK) family, are responsible for connecting transmembrane proteins, such as occludin, claudins, and JAMs, to intracellular actin filaments and the cytoskeleton, ultimately resulting in assembly at TJs.

ZO-1 (220 kDa), which is encoded by the *TJPI* gene, is the first known peripheral protein known with a critical role in the maintenance of TJs and barrier functions [48]. A ZO-1 deficiency leads to defects in angiogenesis and vasculogenesis and a partial loss of TJs [49,50]. ZO-2 (160 kDa) supports ZO-1 and expedites TJ formation and maturation. In particular, ZO-2 is critical during mouse embryonic development [37,51]. Although ZO-3 (130 kDa) is thought to have distinct functions from those of ZO-1 and ZO-2, little is known about this protein [37].

Adherens junctions (AJs), which are formed by VE-cadherin and β -catenin, also constitute junctional complexes and contribute to barrier integrity as modulators by interacting with TJs [36,52]. VE-cadherin specifically upregulates claudin-5 and increases vascular stability by inhibiting FoxO1 activity. In a VE-cadherin-deficient mouse model, molecular permeability across the BBB is increased [53].

2.3. Transport of molecules

One of the critical roles of the BBB is to regulate the transport of molecules across the blood–brain interface [6,52]. The BBB allows the passage of water, blood-dissolved gases, and lipid-soluble substances via passive diffusion, as well as other molecules, such as nutrients that are indispensable for cell survival, through specific transporters. Additionally, ATP-binding cassette (ABC) transporters, called efflux pumps, return cytotoxic or unwanted molecules to the blood to maintain the stable condition of the brain [3,5,22] (Fig. 3).

Small lipophilic molecules, such as oxygen, carbon dioxide, and caffeine, easily enter the brain by passive diffusion through the lipid-rich cell membrane [33]. Similarly, hydrophilic molecules diffuse

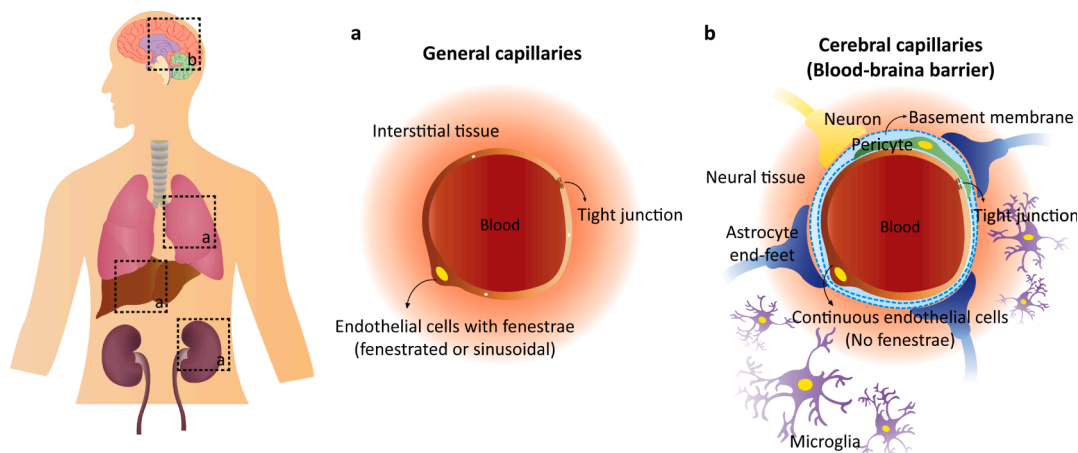


Fig. 1. Structure of the blood–brain barrier. Brain vessels have a distinct vascular structure compared to other organs in the body. (a) In the lung, liver, and kidney, endothelial cells exhibit fenestrae on their surfaces for sufficient molecular transport. (b) Cerebral endothelial cells do not form pores on their soma and form tight junctions with adjacent ECs. The vessels are surrounded by various cell types, including pericytes, astrocytes, neurons, and microglia. Multicellular interactions are indispensable for maintaining brain homeostasis under normal/pathological conditions. Pericytes stabilize blood vessels, and glial cells, including astrocytes and microglia, help maintain barrier properties as critical regulators of neuroinflammation. Neurons control the blood flow in the brain, depending on their metabolic cycle, by neurovascular coupling and contribute to the barrier function of the BBB.

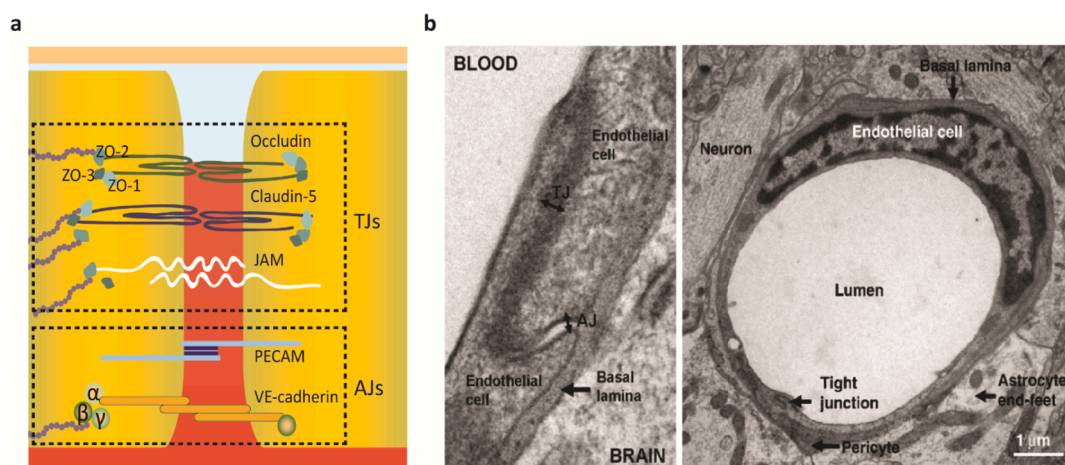


Fig. 2. Structure and components of endothelial tight junctions. (a) In the BBB, cerebral endothelial cells form adherens and tight junctions with neighboring endothelial cells. Tight junctions comprise backbone proteins (occludin, claudin-5, and JAM) and peripheral proteins (zonula occludens 1, 2, and 3). Transmembrane backbone proteins are linked to peripheral proteins, which are bound to actin filaments. Adherens junction proteins (PECAM and VE-cadherin) physically interact with α , β , and γ -catenin. (b) Electron microscopy images of a brain section showing the junctional proteins between endothelial cells. All proteins comprising AJs/TJs are essential for the barrier function in the brain vessel, and the loss of these proteins can lead to BBB dysfunction [41].

across the BBB through the paracellular pathway [32]. Transport *via* passive diffusion is limited to small and highly hydrophobic/lipophilic molecules, which are soluble in water and the hydrophobic part of the lipid bilayer. High lipid solubility and a low molecular weight are the most critical determinants of BBB penetration [54,55]. Molecules able to passively diffuse across the cell membrane have a molecular weight of less than 500 Da [56]. However, highly lipid-soluble molecules are not released from the BBB. Even when lipid-soluble molecules pass through the BBB, they are not released from the surface of endothelium due to their high affinity with ABC efflux transporters. Therefore, for effective transport to the brain, molecules must have proper lipid-solubility ($\log P_{oct}$ in the range of 2–4) [33].

The BBB is selectively permeable and its function is determined by various kinds of transporters expressed on the luminal/abluminal side of endothelial cells [57,58]. The ABC transporters expressed on the abluminal side of the BBB are ATP-dependent efflux pumps. These transporters, which are classified into 48 distinct transporters and 7 families [32], transport toxic metabolites and xenobiotics (such as drugs or neurotoxins) from the brain back to the blood, thereby actively

removing potentially toxic substances located near the BBB [32,33,55,59]. These functions can explain the high multidrug resistance of the BBB [32]. P-glycoprotein (P-gp), a protein encoded by *MDR1* or *ABC1* in humans, is a well-known efflux pump [60]. The drug digoxin accumulates in the brain tissues, with 200-fold higher levels in *mdr1a* P-glycoprotein knockout mice than in control mice [61]. P-gp has a high affinity for diverse substrates, such as aldosterone, doxorubicin, nelfinavir, rhodamine 123, and vecuronium [62]; however, the mechanism by which P-gp interacts with an extensive range of substrates is unclear. Interestingly, P-gp is also responsible for amyloid- β (A β) efflux, which is considered a main regulator of Alzheimer's disease and dementia [63].

Small polar molecules, such as glucose, glutamine, serine, and essential neural amino acids, which are essential for metabolism, pass through the BBB *via* solute carrier-mediated transport [52,64]. There are various groups of SLC transporters, including hexose, monocarboxylic acid, amino acid (neural, anionic, cationic, and beta), choline, nucleoside, and medium-chain fatty acid transport systems [32,65,66]. Glucose transporter (GLUT1), which belongs to the hexose

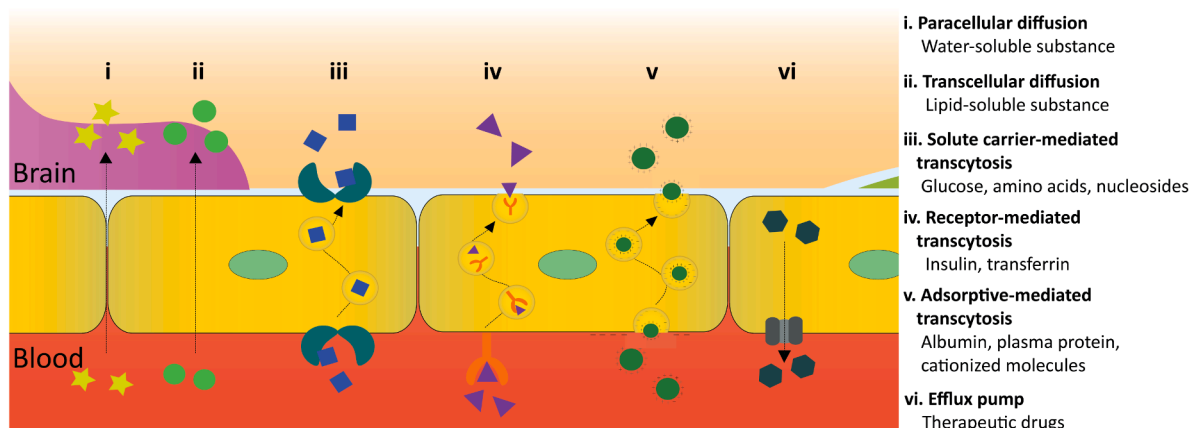


Fig. 3. Molecule transport pathways in the blood–brain barrier. In the brain, paracellular transport is strictly regulated by TJs between endothelial cells. (i) Therefore, a water-soluble substance with a low molecular weight is transported to the neural tissue *via* the paracellular pathway. (ii) Additionally, a lipid-soluble substance passively diffuses through the cell membrane. These two pathways are mediated by a concentration gradient. (iii) The transport of macromolecules, such as metabolic nutrients that are essential for cell growth/survival, is mediated by a specific transport system called solute carrier-mediated transcytosis. (iv) Similarly, insulin and transferrin bind to a specific receptor located on the cell membrane and are transported into the brain. (v) Positively charged substances are absorbed in the cell membrane due to the difference in charges and then transported to the neural tissue. (vi) Efflux pumps, such as P-glycoprotein, excrete toxic/foreign substances or therapeutic drugs, such as antitumor drugs and HIV protease inhibitors, through the BBB.

transport system, is dominantly expressed on the luminal side of brain endothelial cells and transports glucose to the brain by a sodium-independent mechanism [58]. Two types of glucose transporters have been identified: glucose transporter and sodium-glucose transport proteins (SGLT). Normally, glucose is transported by GLUT1 expressed on endothelial cells and is taken up by various cells in the ECM, including neurons, astrocytes, and microglia. The distribution and location of glucose transporters depend on the cell type and physiological conditions [67,68]. The dysregulation of GLUT1 is related to diseases, such as seizures, Alzheimer's disease, and diabetes [69,70]. Amino acid transporters, classified into five groups (system L, γ^+L , x_c^- , asc, and $b^0,+$), also contribute to neuronal function, promoting the synthesis of neurotransmitters, peptides, and proteins [32]. The dysfunction of AA transporters is mainly associated with mental disorders, such as depression and neurological diseases [32,71]. Water-soluble vitamins are carried to brain tissues by diffusion. However, fat-soluble vitamins A, D, E, and K bind to carrier proteins and are then transported to the brain. For example, vitamin D, which is essential for brain development and the modulation of BBB function in stroke, is transferred across the BBB by binding to a vitamin D-binding protein (DBP) [72,73].

Highly limited transcytosis on the cerebral endothelial cells also contributes to the barrier function of the BBB. Compared to endothelial cells isolated from other tissues, such as the lung, major facilitator superfamily domain-containing 2a (*Mfsd2a*), which is associated with BBB formation as a suppressor of transcytosis in the CNS, is highly expressed on brain endothelial cells [74,75]. A variety of non-lipid-soluble macromolecules, such as proteins and peptides, are transported into the brain *via* receptor-mediated transcytosis (RMT) or adsorptive-mediated transcytosis (AMT) [52]. Circulating peptides, such as insulin, transferrin, low-density receptor related protein 1, leptin, immunoglobulin, and angiotensinogen, bind to the luminal side of endothelial cells with high affinity. Transporters include insulin-like growth factor receptor, low-density lipoprotein receptor, and transferrin receptor [32]. RMT requires three steps: (i) internalization, (ii) intracellular movement and sorting, and (iii) exocytosis [74,76]. (i) Macromolecular ligands bind to the receptor on the luminal side and are transported into the endothelium *via* clathrin or caveolae-mediated endocytosis [77,78]. (ii) After they are internalized into cells, they are sorted for transcytosis or degradation at lysosomes. For example, molecules with high affinity for transferrin receptor (TfR) are sorted for degradation and recycling, while molecules with low affinity for TfR are sorted for transcytosis.

Recent studies have shown that this process is regulated by cellular tubules [79,80]. (iii) Lastly, sorting tubules are fused to the carrier organelle and released to the abluminal side [74,76,81]. The molecules must have a cationic surface for transport *via* the AMT. Cationic macromolecules, such as albumin and other plasma proteins, interact with the endothelium, which has a negatively charged membrane. These molecules fuse to the cell membrane and their contents are expelled from cell by a similar mechanism to the RMT [52,82]. The detailed mechanism underlying transcytosis at the BBB remains an open question. Future studies of the regulation of transcytosis are needed, as these transport systems are important for the maintenance of the required concentration gradient and brain homeostasis.

Ions, especially K^+ , Na^+ , and Ca^{2+} , play important roles in neuronal function [83]. Therefore, the ionic concentration gradient among the plasma (luminal side), interstitial fluid (ISF, abluminal side), and cerebrospinal fluid (CSF) must be tightly regulated, since their accumulation in brain tissues can cause critical seizures by hindering neuronal activity [84–86]. The levels of K^+ and Ca^{2+} in the plasma (K^+ : 4.6 mM, Ca^{2+} : 5 mM) are higher than those in the ISF and CSF (K^+ : 2.9 mM, Ca^{2+} : 2.5 mM), while Na^+ concentrations are similar in the plasma (148–155 mM) and CSF (152–156 mM) [83,87,88]. When the ionic concentration gradient is normally maintained, neurons can fire and release neurotransmitters to stimulate other neurons [83,85].

2.4. Physio-pathology of the BBB in brain diseases

In the BBB, two kinds of barrier functions exist: a structure-based physical barrier and active transporter-based biochemical barrier. TJs (VE-cadherin, ZO-1, occludin, and claudin-5) between endothelial cells physically inhibit the entry of macromolecules to the brain. On the other hand, ABCB1, ABCC1–6, and ABCG2 on endothelial cells selectively control the transport of molecules at the interface of the brain and vessels [32,65,66,89]. When the vascular integrity is critically impaired, these barrier functionalities are impaired, resulting in an abnormal ion gradient, the efflux or influx of neuroproteins at the blood vessel–brain interfaces, and even the entry of neurotoxic molecules into the brain tissue [90]. Near the damaged blood vessel, blood-derived neurotoxic molecules accumulate and these deposits of plasma proteins, such as fibrin and thrombin, can cause an inflammatory-like response (Fig. 4) [91,92].

Disruption of the BBB is observed in various neurodegenerative

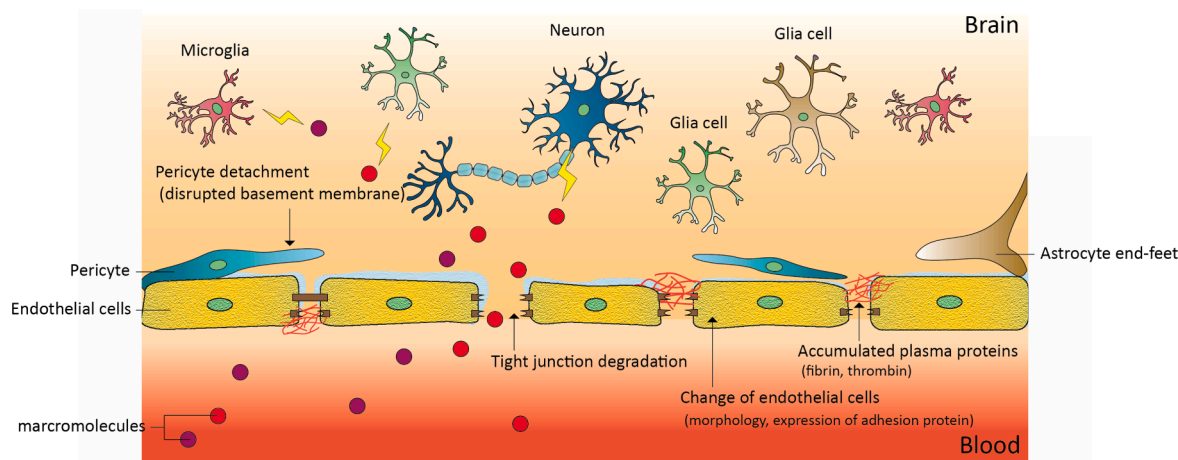


Fig. 4. Disruption of the blood–brain barrier. An impaired BBB structure is frequently observed in various CNS diseases. The pericyte and astrocyte end-feet, which directly contribute to barrier functionality, are detached from the endothelium with a disorganized basement membrane. The pathophysiological condition also disorganizes the basement membrane surrounding the brain endothelium. Tight junctions are degraded and various neuroproteins, such as amyloid-beta and tau, accumulate near the damaged blood vessel. An enlarged gap between endothelial cells results in the entry of unknown molecules to the brain, disrupting homeostasis. Other cells in brain tissues secrete inflammation-associated cytokines and endothelial cells express inflammation-associated markers, such as ICAM-1 and VCAM-1.

brain diseases, like Alzheimer's disease, multiple sclerosis, and Parkinson's disease, and in neuroinflammatory diseases, acting as either causes or consequences [91,93–96]. In the healthy brain, pericytes (which are mural cells of the BBB) cover 80% of brain vessels with a thin plasma membrane. These cells completely block molecules larger than 500 Da from passing through the BBB [89,95,97]. However, in the diseased brain, pericytes are detached from the endothelium and the integrity of junctional proteins (VE-cadherin, ZO-1, occludin, and claudin-5) is lost [98–100]. In APP/PSEN1/*Tau*/Pdgrf β /APOE transgenic models of Alzheimer's disease, BBB breakdown and the loss of pericytes are observed with elevated A β production, limited A β /tau clearance, and neuronal injury [91]. In addition, expression levels of low-density lipoprotein receptor-related protein-1 (LRP-1) and P-glycoprotein, involved in A β clearance, are decreased in the model of Alzheimer's disease. Accumulated amyloid plaques in the brain consequentially promote Alzheimer's disease progression [101]. In ischemic stroke, proinflammatory cytokines (TNF- α and interleukins) are produced and hypoxia-inducible factor-1 α (HIF-1 α) activates matrix metalloproteinases (MMPs), which can degrade TJs, thereby increasing paracellular solute leakage [90,102,103]. Levels of adhesion molecules, such as intercellular adhesion molecule 1 (ICAM-1) and vascular cell adhesion molecule 1 (VCAM-1), which are hardly expressed in normal endothelial cells, increase in response to inflammatory cytokines [104,105]. During ischemia, oxidative stress due to the increased production of reactive oxygen species can lead to BBB injury as well as fatal damage to glial/neuronal cells [90,103].

The disrupted BBB in various CNS diseases is known to accelerate disease progression via the accumulation of inflammatory or toxic molecules in brain tissues. Accordingly, extensive research has focused on the development of therapeutic strategies aimed at BBB protection. For example, 4-hydroxy-2,2,6,6-tetramethylpiperidine-N-oxyl (TEMPO), an antioxidant drug, has been investigated for the prevention of hypoxia-reoxygenation (H/R)-induced ROS damage and for the prevention of the disruption of occludin assembly [90]. For CNS-associated diseases, a large library of drug candidates has to be tested with respect to efficacy. To decouple the effects of various biochemical parameters and to monitor drug effects, organ-on-a-chip technology has recently emerged as an advanced and powerful platform.

3. Contributions of various cellular components to BBB function

Three main cellular components, cerebral endothelial cells, astrocytes, and pericytes, contribute to BBB function and are regulated by

distinct mechanisms [106]. In the following sections, the specific roles of each cellular component in the regulation of BBB function are reviewed.

3.1. Cerebral endothelial cells

Endothelial cells within the brain tissue have similar and distinct features compared with endothelial cells located in other organs [25,107]. Cerebral endothelial cells respond to a variety of biological factors associated with the control of the vascular tone or diameter in a similar manner to endothelial cells in other tissues [4,10]. The unique properties of brain endothelial cells are as follows: (1) a lack of fenestrae in the cell body, (2) a low vesicle content in the cytoplasm, (3) a high density of mitochondria, and (4) higher expression of TJ proteins [25,108].

Generally, endothelial cells are classified into three types, fenestrated, sinusoidal, and continuous endothelial cells, depending on their physical properties [107]. In the case of endothelial cells in organs other than the brain, molecules are transported through the fenestrae on their surfaces to facilitate mass transport between the blood and interstitial tissue [109,110]. In the kidney, liver, intestinal tract, and endocrine organs, the fenestrated and/or sinusoidal endothelial cells have pores and are highly permeable to water and large solutes [25,107]. Continuous endothelial cells, which are predominantly observed in the BBB, have no fenestrae on their surfaces, therefore allowing the entry of only small molecules that are soluble in water into the CNS through intercellular gaps and the cell membrane [25]. In addition, cerebral endothelial cells possess fewer vesicles within the cytoplasm compared to endothelial cells in other organs [111]. Due to the absence of pores, the limited amount of vesicles, and the presence of TJs, the transport of molecules through para- and transcellular pathways is strictly limited [112–114].

3.2. Astrocytes

Many types of glial cells are present in the brain, such as astrocytes, oligodendrocytes, and microglia, and they account for over 90% of the total cell number, depending on the brain region [7,115]. Among glial cells, astrocytes are the most abundant and are located in closest spatial proximity to the cerebral endothelium [116,117]. In the CNS, two main types of astrocyte exist: protoplasmic astrocytes in the gray matter and fibrous astrocytes in the white matter. Protoplasmic astrocytes have fewer fibrils and extend several branches that encase the neural soma

and synapse. Fibrous astrocytes interact with oligodendroglial cells and the nodes of Ranvier, forming contacts through their long fiber-like branches [118–120].

Both types of astrocytes contact the blood vessel and regulate vascular functions [116,121]. Astrocytes encircle the abluminal side of the endothelium by anchoring their polarized end-feet towards endothelial cells. Due to the close anatomical locations of astrocytes and endothelial cells, researchers have hypothesized that astrocytes play an important role in maintaining the BBB phenotype [122]. In fact, their end-feet express the water channel aquaporin 4 (AQP4) and potassium channel Kir4, and these water and ion channels regulate water and ion homeostasis [123–125]. The end-feet also express protein transporters, including glucose transporter-1 and P-gp [121]. According to several *in vivo* and *in vitro* studies, astrocytes are responsible for maintaining the BBB, enhancing the barrier function, and restoring the action of barrier function after damage to brain tissues [126]. When astrocytes are implanted near leaky vessels, they tighten the vessel and restore vascular impermeability [127]. Furthermore, astrocytes induce and enhance the BBB phenotype (e.g., selective permeability, tight junction protein expression, and specific transport systems) of primary and immortalized endothelial cells, indicating that they enhance the barrier properties *via* cross-talk with the endothelium in the brain [128,129]. Astrocytes release several factors, such as sonic hedgehog (SHH), angiotensin I&II (ANG-I&II), and apolipoprotein E (APOE) [130–132]. SHH secreted by immature astrocytes increases the expression of occludin and claudin-5. ANG-I&II, which are ligands for receptors expressed on endothelial cells, such as Tie2 and angiotensin type 1 receptor (AT1), upregulate TJ protein expression and decrease paracellular transport [6]. APOE interacts with the low-density lipoprotein (LDL) receptor and contributes to not only to the maintenance of BBB functions but also the restoration of barrier integrity after injury. This process is summarized in Fig. 5. In angiotensinogen (AGT)- or APOE-deficient models, levels of TJ proteins are reduced and paracellular leakage across the BBB occurs [133,134]. Moreover, Src-suppressed C-kinase substrate (SSECKS) derived from astrocytes suppresses the expression of vascular endothelial growth factor (VEGF), which is known to promote blood vessel formation. Furthermore, the inhibition of JnK phosphorylation reinforces TJs and increases the impermeability of the BBB [135]. Astrocytic laminins (laminins-111 and -211), which are exclusively produced by astrocytes in the brain, influence BBB stability by controlling the differentiation of

pericytes [136].

Astrocytes are also regarded as central regulators of the immune response to pathological conditions in the CNS. These cells respond to cytotoxic and inflammatory substances, produce various cytokines, and ultimately activate immune cells to exacerbate tissue damage and promote repair [137–139]. According to recent studies, the neuroprotective signaling pathways in astrocytes are triggered by cytokines, growth factors, and hormones during neuroinflammation [137].

3.3. Pericytes

Contractile cells located near blood vessels were discovered by Rouget in 1873 [140–142]. Later, Zimmermann named these cells “pericytes,” implying their prominent location close to endothelial cells [143]. Although pericytes have attracted increasing attention, our understanding of their physiological functions is limited owing to the lack of a specific single marker for this cell type [144]. Pericytes have been described as smooth muscle cells, perivascular fibroblasts, and perivascular mesenchymal stem cells based on their expression of contractile fibers, perivascular location, and trans-differentiation and tissue regeneration ability [145]. However, recent studies have indicated that pericytes express high levels of platelet-derived growth factor receptor- β and interact with endothelial cells *via* platelet-derived growth factor-BB (PDGF-BB) signaling in the vascular basement membrane. This means that pericytes have a distinct identity from vascular smooth muscle cells, fibroblasts, and other perivascular cells [146,147].

In the brain, pericytes wrap around the endothelial cells embedded within the basement membrane and interact with cerebral endothelial cells *via* both direct contacts, forming ‘peg-and-socket’ junction, and paracrine signaling [106,148,149]. Pericytes are present at a higher density in the brain than in other tissues and are thought to regulate blood flow through their contractility [6,146,148]. These cells contract and dilate in response to vasoactive stimuli, such as ischemia, to redistribute the blood flow by locally controlling the diameter of capillaries [150]. In addition, pericytes also play roles in the formation and maintenance of the BBB and revascularization of impaired vessels [6,149]. In the angiogenic sprouting model, endothelial cells are recruited by biochemical factors secreted by pericytes, and pericytes prohibit further invasion of endothelial cells following the establishment of direct contacts. Thus, pericytes are implicated in the modulation of angio- and vasculogenesis [151,152]. For example, adhesion between platelet-derived growth factor receptor- β (PDGFR- β) on pericytes and platelet-derived growth factor (PDGF-B) on endothelial cells have recently been reported to regulate the recruitment of pericytes and their attachment to the endothelium [148].

Pericytes have different effects on BBB integrity, depending on their differentiation stage. Thanabalasundaram et al. showed that pericytes differentiated under different conditions (i.e., serum-free medium supplemented with TGF β or bFGF) show differences in morphology (+ TGF β : large cell body; + bFGF: small cell body), proliferation rates, and the expression of pericyte markers (α -SMA, desmin, and nestin) and permeability factors (VEGF, MMP-2, and MMP-9). The coculture of endothelial cells with bFGF-pretreated pericytes resulted in the highest TEER and claudin-5 expression. These results are further supported by the low secretion of permeability factors. In other words, in the resting state, pericytes with small cell bodies express a low level of the contractile protein α -SMA and thus stabilize BBB integrity. However, pericytes in the contractile state have long fibers through their enlarged cell bodies and impair the barrier function of the BBB *via* the elevated secretion of permeability factors [153].

As mentioned above, pericyte identity, contractile function, and roles in physiological & pathological states remain open questions. To define their identity and distinguish them from other cells, the identification of pericyte-specific markers is needed.

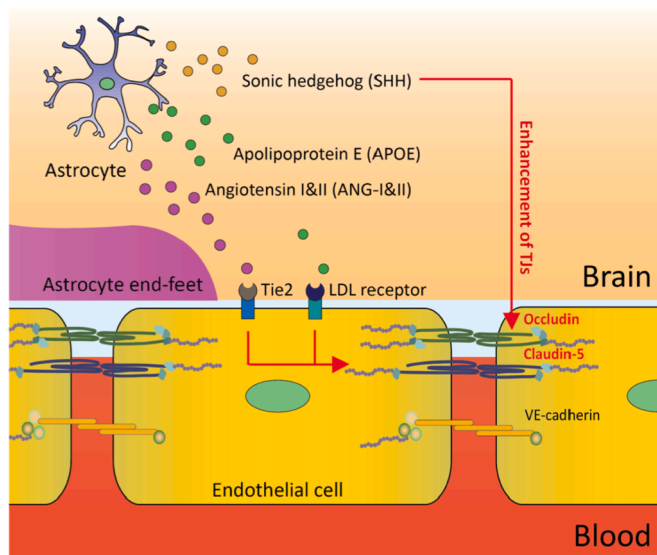


Fig. 5. Contribution of astrocytes to BBB integrity. Astrocytes secrete various cytokines, such as sonic hedgehog, apolipoprotein E, and angiotensin I&II, to regulate BBB function. Secreted cytokines interact with endothelial cells by binding to the specific receptor and promote the synthesis of tight junctions.

3.4. Extracellular matrix

The ECM secreted by surrounding cells has diverse functions as a biomechanical scaffold, including the introduction of physical tension and anchoring points, the control of molecular transport, and the regulation of regenerative/degenerative processes [154–156]. The interstitial matrix present between cells and the basement membrane are also part of the ECM. Compared to other organs, the brain has small amounts of fibrous proteins, such as collagen and fibronectin [157]. Instead, the brain contains numerous hyaluronic acids (HA) and various proteoglycans (aggrecan, versican, brevican, and neurocan) [156,157]. Sulfated glycosaminoglycans form proteoglycans (hyaluronan, chondroitin sulfate, dermatan sulfate, heparan sulfate, and keratan sulfate) by binding to the core protein. HAs, unique unsulfated glycosaminoglycans, noncovalently interact with these proteins and establish a stable multimeric matrix. HA stimulates cellular signaling pathways that induce invasion and migration by binding to the cell surface receptors CD44 and hyaluronan-mediated motility receptor (RHAMM) [33,158]. Furthermore, HA exhibits a high hydration capacity *in vivo* and it is widely used as a cell encapsulation material *in vivo* by injection [159,160]. Lecticans, including aggrecan, versican, brevican, and neurocan, possess an HA-binding domain. Lecticans interact with surrounding cells and growth factors and affect neuronal functions [157,161]. Neurocan, which is only expressed in the nervous tissue, inhibits neurite outgrowth. Versican promotes neuronal cell adhesion and axon growth [156,157].

In the CNS, endothelial cells are embedded in the 50–100-nm-thick basement membrane consisting of laminin, fibronectin, and collagen type IV [33]. Laminin is involved in regulating the polarization of epithelial cells [162]. Fibronectin binds the ECM components together as a major adhesive protein and facilitates cell adhesion, growth, and differentiation. Fibronectin is also necessary for wound healing and embryogenesis [163]. Collagen type IV serves as a supporting component of the basement membrane and interacts with endothelial cells [164]. When endothelial cells are grown in a mixture of these proteins *in vitro*, they display a high TEER value, revealing the imperative roles of the cerebral basement membrane in vascular stability and barrier functions [165].

A summary of the types and functions of basement membrane proteins is provided in Table 1.

3.5. Biophysical environment in the BBB

In the BBB, endothelial cells are exposed to two kinds of biophysical cues, including nanoscale topography and fluidic shear stress on the apical and basal side [167]. On the apical side of the vessel, the endothelial cells are covered with the basement membrane composed of a complex of various proteins, such as laminin, collagen type, and fibronectin [168]. Since these crosslinked fibers allow the formation of nanostructures on the apical surface of the vessel, the endothelial cells are affected by the specialized topographical surface. The biomimetic topography contributes to cell behaviors, including orientation/elongation, proliferation, and migration [169–171].

Table 1

Types and functions of basement membrane proteins in the BBB.

Basement membrane protein	Functions	Properties	Ref.
Laminin	<ul style="list-style-type: none"> Regulates epithelial cell polarization 	<ul style="list-style-type: none"> Composed of three different polypeptide chains Associated with type IV collagen network 	[121] [166]
Fibronectin	<ul style="list-style-type: none"> Binds ECM components as a major adhesive protein Facilitates cell adhesion, growth, and differentiation Related to wound healing and embryogenesis 	<ul style="list-style-type: none"> Protein dimer of very similar units of 220–250 kDa Binds to collagen 	[122] [166]
Collagen type IV	<ul style="list-style-type: none"> Supporting component of the basement membrane Interacts with endothelial cells 	<ul style="list-style-type: none"> Major component of basement membranes Consists of three polypeptide chains 	[123] [166]

On the basal side of the vessel, the endothelial cells are exposed to fluidic shear stress caused by circulating blood. Shear stress generated from the laminar flow is a critical factor affecting the endothelial cell polarity and barrier properties of the BBB. The value of shear stress in cerebral capillaries ranges from 0.01 to 10 dyn/cm². In particular, physiological shear stress (6 dyn/cm²) is known to increase the expression of TJ/AJ-related RNAs, drug efflux transporter genes, as well as the TEER value [36,172]. In addition, fluidic shear stress promotes cellular adhesion to the extracellular matrix by increasing integrin-ligand binding [173]. Furthermore, it induces cell alignment in the direction of the blood flow and increases the localization of TJ proteins at the cell–cell junctions by the reorganization of the cytoskeleton [174].

4. Advances in the development of *in vitro* blood–brain barrier models

Over the last few years, various types of *in vitro* microvasculature models have been reported. These models exhibit promising characteristics for a wide range of basic science applications, such as vascular function and angiogenesis, and clinical applications, such as drug screening [20]. Recently, with the help of commercially available primary and immortalized cells originating from the brain, revolutionary *in vitro* BBB models have been fabricated. These models are classified into four general types: (i) the Transwell, a conventional *in vitro* model, (ii) the microfluidic chip in which a porous membrane or micro-post is embedded, (iii) the spheroid-based approach, and (iv) the hydrogel-laden microfluidic chip (Fig. 6). In the following sections, recent advances in the development of *in vitro* BBB models are reviewed. Recent research has focused on not only mimicking the *in vivo* BBB environment but also on its application as a model for disease or transport (drugs, antibodies, or other molecules) studies. Thus, the scope of applications in the biomedical field is considered a crucial factor for evaluating the usefulness of an *in vitro* platform. From this perspective, we selected representative examples in each category.

Types of *in vitro* BBB models and representative examples are outlined in Tables 2 and 3.

4.1. Transwell model

Transwell assays are widely used to monitor cellular invasion/migration and to analyze molecular transport. Transwell systems are composed of two chambers separated by a porous membrane. Cerebral endothelial cells are plated on the membrane coated with basement membrane proteins, including fibronectin, laminin, and collagen, and optionally cocultured with other cell types, such as astrocytes, pericytes, and neurons, to mimic the BBB properties. Glial cells and perivascular cells are generally cultured on opposite sides of the membrane or in the bottom chamber (Fig. 6a). The physical barrier function of this simplified BBB model is evaluated by measuring the TEER between two chambers or by measuring the paracellular permeability of fluorescently labeled solutes. In the case of TEER measurements, one electrode is placed in the top/apical side and the other electrode is inserted into the bottom/basolateral side [200]. For transport assays, the

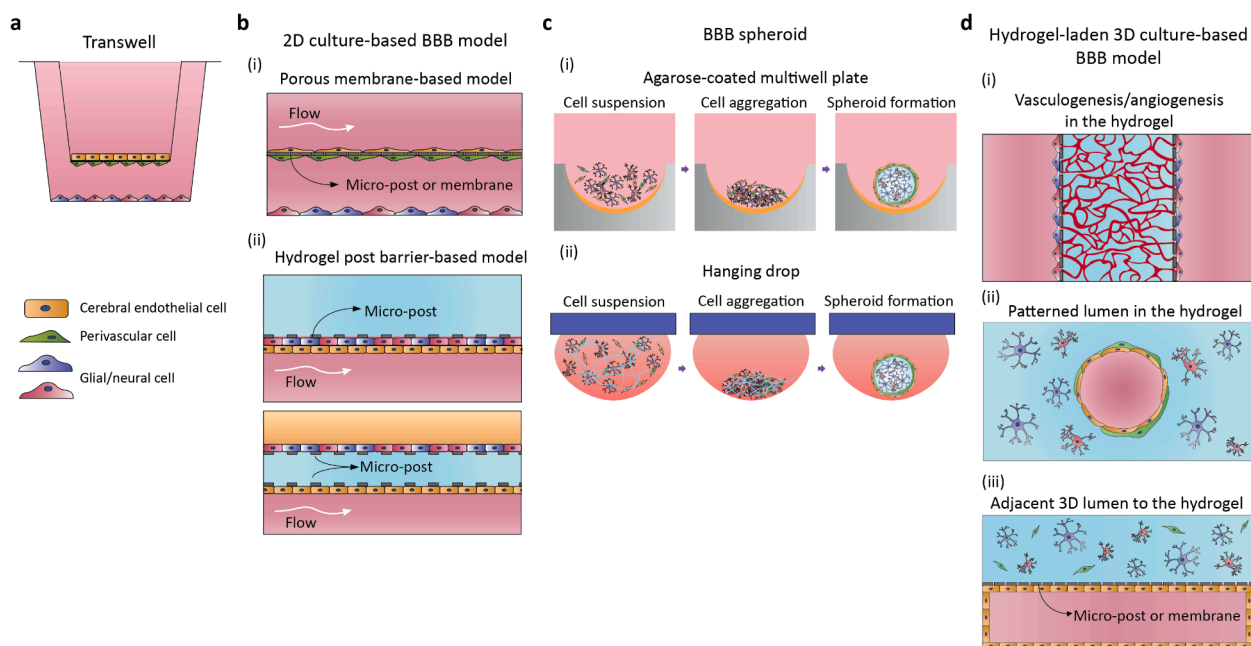


Fig. 6. Classification of *in vitro* BBB models. Various types of BBB models have been developed to recapitulate the structure and physiology of the BBB *in vivo*. (a) Transwell systems are widely used owing to their simplicity, reproducibility, and high-throughput screening capability. Endothelial cells are cultured on the porous membrane and other supporting cells are cultured on the opposite side or in the output chamber. (b) A perfusion-integrated 2D-based microfluidic model. Endothelial cells are cultured on the porous membrane or hydrogel surface and then continuously exposed to fluidic shear stress. (c) In the case of BBB spheroids, cells of the BBB (endothelial cells, pericytes, and astrocytes) spontaneously organize into spheroids on the low-attachment culture vessel or on the microwell array. (d) As an improved 3D model, the hydrogel-laden microfluidics platform mimics the 3D microenvironment of perivascular cells and neural/glial cells, since they are embedded in the bulk hydrogel. Two approaches have been used to fabricate the vasculature in the hydrogel: bottom-up (vasculogenesis/angiogenesis in the hydrogel) and top-down (viscous fingering patterning, removing the templates from the gel, and patterned microvasculature).

fluorescently labeled solute is allowed to infuse from the top/apical side to the bottom/basolateral side, and time-dependent changes in intensity are measured on the bottom. The difference in the fluorescent intensity between the two chambers is determined, depending on TJ formation [201]. *Ready-To-Use BBB Kit™*, which is commercially available from *PharmaCo-Cell Company (Tokyo, Japan)*, is a Transwell-based *in vitro* cell culture platform for mimicking the BBB and monitoring drug transport. There are two kinds of membrane materials (polyethylene terephthalate and polyester) with different pore sizes (3.0 μm and 0.4 μm) and pore densities (2×10^6 pores/cm 2 and 4×10^6 pores/cm 2).

The Transwell system has several advantages, such as the ease of handling, cost-effectiveness, ease of measuring TEER, and potential for parallel and high-throughput screening. To measure TEER in an animal model, an amplifier-integrated complex system for delivering the current with the proper frequency and measuring the potential profile is required. TEER can be calculated based on the theory developed by Crone & Olesen in 1982 by using various parameters including the resistivity of blood, radius of the vessel, vessel cross-sectional area, and length constant [202,203]. Although TEER measurement is easier in the Transwell model, the values (TEER and permeability) differ between *in vivo* (TEER: $> 1500 \Omega \text{ cm}^2$, permeability: $< 10^{-6} \text{ cm/s}$) and Transwell (TEER: $\sim 300 \Omega \text{ cm}^2$, permeability: $\sim 10^{-5} \text{ cm/s}$) conditions, implying the need for further improvements to mimic BBB functions. Indeed, the Transwell membrane has different pore sizes and a thickness of 10 μm , which is 300 times thicker than the natural basement membrane observed in the vascular structure, limiting direct physical contacts among cells through the pores. Furthermore, the porous membrane is inherently two-dimensional and utilizes a stiff polymeric material, such as polycarbonate (elastic modulus of $\sim 2 \text{ GPa}$), substantially different from *in vivo* conditions. The absence of a fluidic condition is also a limitation of the Transwell system. Therefore, a substantially improved BBB system is needed to replicate *in vivo* BBB physiology, including the

fluidic circulation for endothelial polarization, 3D structure, physiologically relevant mechanical properties, and composition of the ECM [19,33].

4.2. 2D culture-based BBB models

Blood always circulates along a vessel in the body to supply oxygen and nutrients to the tissue and remove carbon dioxide and metabolic waste. In this continuously circulating environment, endothelial cells are consistently exposed to fluidic shear stress and adapt their morphology, phenotype, cytokine secretion, and signaling in response to the fluidic environment. According to *in vitro* assays, fluidic shear stress increases cell proliferation, migration, the levels of TJ/AJ proteins in ECs, and cell-ECM adhesion [172,174]. For these reasons, flow-induced shear stress has been regarded as an essential factor for mimicking *in vivo* BBB characteristics. As a result, diverse types of BBB models integrating shear stress have been developed. These models have common features of an endothelial monolayer growing on a porous membrane sandwiched between two microchannels (luminal and abluminal sides). Hydrogel injection to the ECM channel separated by micro-posts prevent the gel from entering the side channels. The endothelial cells and glial/neuronal cells are directly or separately cultured on the surface of the hydrogel. Finally, the vascular channel is connected to a syringe or peristaltic pump that continuously applies fluidic shear stress to the endothelial cells (Fig. 6b).

Wang et al. [183] cocultured an immortalized mouse brain endothelial cell line (b.End3) on one side of the porous membrane and mouse astrocytes and pericytes on the opposite side, which was then sandwiched between the microchannels (Fig. 7a). When the culture medium is pumped into the device, the cultured endothelial cells are exposed to a fluidic shear stress of 1.6 dyn/cm 2 . In their design, high viability and *in vivo*-like low paracellular permeability of [^{14}C]-mannitol and [^{14}C]-urea were detected in bi- and triculture models for up to

Table 2
Summary of features of *in vitro* BBB models.

Model	Principle	Merits	Limitations
Transwell	<ul style="list-style-type: none"> ● Cells are separately cultured on both sides of a porous membrane ● Cells are cultured under a static environment 	<ul style="list-style-type: none"> ● Simplicity ● Easy measurement of TEER ● High throughput 	<ul style="list-style-type: none"> ● 2D culture on a stiff membrane ● No fluidic shear stress ● No 3D ECM ● Low relevance to <i>in vivo</i> conditions (e.g., low TEER, high permeability)
2D culture-based model	<p>< Porous membrane-based model ></p> <ul style="list-style-type: none"> ● A porous membrane is sandwiched between two PDMS layers with microchannels ● Cells are separately cultured on both sides of a porous membrane ● Pump can be connected to vascular channels for fluidic shear stress <p>< Hydrogel barrier post-based model ></p> <ul style="list-style-type: none"> ● Hydrogel is injected to the ECM channel ● Cells are separately cultured on the surface of the hydrogel ● Pump can be connected to vascular channels for fluidic shear stress 	<ul style="list-style-type: none"> ● Fluidic culture ● Ease of fabrication 	<ul style="list-style-type: none"> ● Planar organization of (2D) cell culture on the membrane ● No 3D ECM
Spheroid model	<p>< Non-adhesive cell culture ></p> <ul style="list-style-type: none"> ● Mixture of several cells are plated on non-adherent microwells ● Cells spontaneously form a spheroid <p>< Hanging drop ></p> <ul style="list-style-type: none"> ● A drop of cell suspension is placed on a Petri dish ● Dish is inverted ● Cells spontaneously form a spheroid within the droplet 	<ul style="list-style-type: none"> ● Compact 3D structure ● Enhanced cellular interactions <i>via</i> direct contact among cells ● High throughput 	<ul style="list-style-type: none"> ● Development of a hypoxic core ● Inability to monitor the submarginal region due to reduced transparency ● Hard to measure TEER ● Lack of vascular structure
Hydrogel-laden 3D culture-based BBB models	<p>< Self-organization ></p> <ul style="list-style-type: none"> ● Endothelial cells are mixed in angiogenesis-promoting hydrogels such as a fibrin gel w/or w/o other cells ● Endothelial cells spontaneously form vessels within the 3D gel <p>< Viscous fingering ></p> <ul style="list-style-type: none"> ● Medium is infused to the pre-gelled hydrogel ● Due to the difference in viscosity, a hollow channel is formed ● Endothelial cells are seeded on the luminal surface of the channel <p>< Patterned lumen ></p> <ul style="list-style-type: none"> ● A microneedle is removed from the gelled hydrogel ● Endothelial cells are seeded on the luminal surface of the channel <p>< Phase guide ></p> <ul style="list-style-type: none"> ● Hydrogel embedded w/or w/o cells is injected to the chamber surrounded by a micro-post array or physical barriers, which inhibit liquid spreading ● Endothelial cells are seeded on the gelled hydrogel surface 	<ul style="list-style-type: none"> ● 3D culture environment ● <i>In vivo</i> ECM-like microenvironment ● Fluidic culture conditions 	<ul style="list-style-type: none"> ● Complexity ● Hard to measure TEER ● Low throughput

21 days. [³H]-Dexamethasone, a substrate of P-gp, was infused into the channel to confirm the pumping activity of the BBB, and its basolateral-to-apical transport gradually increased, proving the functionality of the efflux pump in the endothelial cells. Using a similar approach, Wang et al. [182] designed a pumpless microfluidic BBB model characterized by low complexity and convenience (Fig. 7b). The neural chamber and flow rate were scaled down based on the fluid-to-tissue volume ratio and residence time of fluid in a human adult brain. Gravity-driven flow was induced using a rocking platform, and recirculation was achieved by changing the tilting direction. Human induced pluripotent stem cell (iPSC)-derived brain microvascular endothelial cells (BMECs) were cocultured on the collagen IV- and fibronectin-coated porous cell insert with primary rat astrocytes. This model exhibited high TEER values (peak value: $4399 \pm 242 \Omega \text{ cm}^2$) and low permeability to various model molecules (4, 20, and 70 kDa FITC-dextran) and small drugs (caffeine, cimetidine, and doxorubicin), and the results were strongly correlated with *in vivo* data.

The reported BBB models can be further developed as disease models. Xu et al. [178] utilized their BBB model to monitor the process of brain metastasis and screen the therapeutic response to anti-cancer agents (Fig. 7c). Primary rat astrocytes and endothelial cells were seeded on the collagen-coated surface and cultured in a dynamic environment. The authors injected several tumor cells into the vascular part and confirmed the selective brain metastasis of lung cancer, breast cancer, and melanoma, which are known to have a high propensity to

metastasize to the brain *in vivo*. For drug screening, temozolomide (TMZ), a BBB-permeable anti-glioblastoma drug, was infused into the vascular channel and led to the apoptosis of brain tumor cells across the BBB, showing the potential of the BBB chip to serve as an anticancer drug screening model. This brain tumor-BBB hybrid model can be applied to fundamental studies of the mechanism of tumor growth and metastasis at the cellular level and the development of efficient drugs or therapies for cancer. Wevers et al. [179] integrated the BBB microfluidic model into an antibody transcytosis assay (Fig. 7d). The authors infused MEM-189, which binds to the human transferrin receptor (hTfR) expressed on endothelial cells, into the microvessel channel. The antibody was transported to the gel chamber by receptor-mediated transcytosis. Recently, Maoz et al. [185] developed an *in vitro* human neurovascular unit by linking the perivascular part (BBB) and brain part (neuronal cells) (Fig. 7e). The authors compared the levels of proteins related to metabolism, immunity, and cell signaling in the coupled/uncoupled system and revealed the effect of multicellular interactions on maintaining brain function. As a personalized iPSC-based BBB model, Vatine et al. [204,205] cultured patient (Huntington's disease and Allen Herndon Syndrome)-specific iPSC-derived neural progenitor cells and brain endothelial cells in the separated channels. They observed the effects of genetic mutations on neuronal activity and vascular function based on calcium imaging, permeability, and TEER monitoring. In the MCT8-mutated and patient-derived BBB model, T3 hormone is blocked from entering the BBB with low permeability

Table 3
Recent advances in the development of *in vitro* BBB models.

Model	Cell type	TEER (Ωcm^2)	Permeability	Experimental results	Ref.
Transwell	Human iPSC-derived brain microvascular endothelial cells, human neural progenitor cells, human brain pericytes, human foreskin fibroblasts	5350 \pm 250	Sucrose: $5.3 \pm 1.7 \times 10^{-7}$ cm/s	Enhanced BBB phenotype following retinoic acid treatment	[175]
	Human iPSC-derived endothelial cells, hiPSC-derived astrocytes, hiPSC-derived pericytes, neural stem cells	2556	Lucifer yellow: 1.58 ± 0.40 $\mu\text{m}/\text{min}$ Fluorescein: 1.33 ± 0.29 $\mu\text{m}/\text{min}$ 4 kDa: 0.0106 ± 0.0016 $\mu\text{m}/\text{min}$ 40 kDa: 0.0030 ± 0.0004 $\mu\text{m}/\text{min}$ Sodium fluorescein: $2.6 \pm 0.4 \times 10^{-6}$ cm/s	Paracellular transport studies with various molecules	[176]
	Human iPSC-derived endothelial cells, hiPSC-derived astrocytes	232.8 \pm 33.1	Not quantified	Verifying the effect of anti-cancer drugs and the A β clearance capacity	[177]
2D culture-based model	Primary rat brain microvascular endothelial cells (BMECs), primary rat cerebral astrocytes	~1298 \pm 86	MEM-189: 1.6×10^{-5} cm/min	Brain metastasis of cancer cells (lung cancer, breast cancer, melanoma, and liver cancer)	[178]
	Human brain microvascular endothelial cells (TY10 cell line), human brain pericytes (hBPCT cell line), human astrocytes (hAst cell line)	~4480 \pm 0.79	3 kDa: 1.5×10^{-5} cm/s, 10 kDa: 5×10^{-6} cm/s, 70 kDa: 3×10^{-6} cm/s	Assessment of antibody transcytosis across the BBB	[179]
	Primary mouse brain microvascular endothelial cells and primary mouse astrocytes	250	4 kDa: 1×10^{-5} cm/s	Real-time drug response monitoring in a multichannel system	[180]
	Immortalized mouse brain endothelial cell line (b.End3), mouse astrocyte cell line (C8D1A)	~4399 \pm 242	20 kDa: 1×10^{-5} cm/s, 70 kDa: 1×10^{-6} cm/s, propidium iodide: 7×10^{-5} cm/s	Monitoring the BBB properties in real-time following exposure to histamine	[181]
Spheroid model	Human iPSC-derived brain microvascular endothelial cells (BMECs) and rat primary astrocytes	~322	4 kDa: 10^{-7} cm/s, 20 kDa: 9×10^{-7} cm/s, 70 kDa: 10^{-8} cm/s	Selective permeability of tracers and drugs (caffeine, cimetidine, and doxorubicin)	[182]
	Immortalized mouse brain endothelial cell line (b.End3), immortalized mouse pericytes, mouse astrocytes (C8-D1A)	~322	Mannitol: 0.3×10^{-6} cm/s, Urea: 0.9×10^{-6} cm/s	Assessment of the function of the P-glycoprotein efflux pump	[183]
	Immortalized mouse brain endothelial cell line (b.End3), immortalized murine astrocytes (C8-D1A), immortalized murine microglia (BV-2), immortalized murine brain neuroblastoma cells (Neuro-2a)	-	-	Measuring the neurotoxic effects of organophosphate <i>in vitro</i>	[184]
	Human hippocampal neural stem cells (HIP-009 cells), cortical human brain microvascular endothelial cells (hBMVECs), human astrocytes, human brain pericytes	-	530 Da: $11.2 \pm 0.8 \times 10^{-6}$ cm/s, 67 kDa: $2.7 \pm 0.2 \times 10^{-7}$ cm/s	Evaluation of drug penetrance and metabolism between the BBB and neurons	[185]
Spheroid model	Primary neonatal rat brain capillary endothelial cells (RBECs), primary neonatal rat astrocytes	-	40 kDa: $1.1 \pm 0.4 \times 10^{-6}$ cm/s	Identifying the barrier function of the neonatal BBB	[186]
	Human cerebral astrocytes (hpAs), human brain vascular pericytes (hpPs), primary human brain microvascular endothelial cells (hpBECs)	-	-	Surface expression of cellular adhesion molecules and receptors	[187]
	Primary cells derived from the postnatal rodent cortex	-	-	Formation of capillary-like networks in BBB spheroids	[188]
	Primary human astrocytes, human brain vascular pericytes (HBVPs), human cerebral microvascular endothelial cell line D3 (hCMEC/D3), primary human brain microvascular endothelial cells (HBMECs)	-	-	Screening of a BBB-penetrating drug (BKM120), dabrafenib (a nonpenetrating drug), and CPPs (cell-penetrating peptides)	[189]
Primary human brain microvascular endothelial cells, primary human brain microvascular pericytes (HBVPs), human astrocytes (HA), human iPSC-derived oligodendrocyte progenitor cells (HO), human iPSC-derived microglia (HM), human iPSC-derived neural stem cells	-	-	Assessment of the effects of MPTP, MPP+, and mercury chloride as indicators of the charge selectivity of the BBB	[190]	

(continued on next page)

Table 3 (continued)

Model	Cell type	TEER (Ωcm^2)	Permeability	Experimental results	Ref.
Hydrogel-laden 3D culture-based BBB models	Human iPSC-derived endothelial cells, human brain pericytes, human brain astrocytes	-	10 kDa: 2.2×10^{-7} cm/s 40 kDa: 0.89×10^{-7} cm/s	Self-assembled microvasculature in contact with pericytes and astrocytes	[191]
	Primary cortical neurons, primary cortical astrocytes, human umbilical vein endothelial cells (HUVVEC), human cerebral microvascular endothelial cells (hCMEC/D3)	-	10 kDa: 2×10^{-5} cm/s 70 kDa: 10^{-5} cm/s	Morphological assessment of primary neurons and size-selective permeability of the BBB model <i>in vitro</i>	[192]
	Human umbilical vein endothelial cells (HUVVECs), astrocytes, neurons	-	20 kDa: $0.45 \pm 0.11 \times 10^{-6}$ cm/s 70 kDa: $0.36 \pm 0.05 \times 10^{-6}$ cm/s	Direct contact between astrocytes and the vascular network	[193]
	Human brain microvascular endothelial cells (hBMVECs), human brain pericytes, human astrocytes	Not quantified	3 kDa: 2×10^{-6} cm/s	Evaluating the function of the BBB model	[194]
	H9-derived human neural stem cells, human brain microvascular endothelial cells (BMVECs), human mesenchymal stem cells (MSCs)	-	-	Optimization triculture of NSCs, BMVECs and MSCs in fibrin, a fibrin-Matrigel mixed gel, and fibrin-hyaluronan mixed gel	[195]
	Human astrocytes, human cerebral microvascular endothelial cells (hCMEC/D3)	-	4 kDa: 0.7×10^{-6} cm/s	Effect of mechanical stimulation (shear stress, cyclic strain, and pulsatile flow) on BBB formation	[196]
	Primary human brain-derived microvascular endothelial cells (hBMVECs), primary human pericytes, primary human astrocytes, human cortical glutamatergic neurons	~6045	-	Identifying barrier integrity in the NVU	[197]
	Rat brain endothelial cells (RBE4), human umbilical vein endothelial cells (HUVVEC), human neutrophils	-	-	Screening the protective effects of drugs on the BBB	[198]
	Immortalized mouse brain endothelial cell line (b.End3)	-	-	Fabrication of an engineered cylindrical brain vascular structure	[199]
	Human iPSC-derived brain microvascular endothelial cells	-	-	Hyperosmolar BBB opening, verifying the neuroinflammatory response and the function of efflux pump, assessing endothelial cell behaviors	[24]
				Lucifer yellow: $2.84 \pm 0.41 \times 10^{-7}$ cm/s Rhodamine 123: $6.61 \pm 0.26 \times 10^{-7}$ cm/s 10 kDa: below the detection limit	

($\sim 10^{-6}$ cm/s), as observed in patients, while the MCT8-corrected BBB and normal model showed healthy vascular function. This example clearly displays the usefulness of the patient-derived BBB model for studies of patient-specific pathophysiology.

Several kinds of commercially available microfluidic cell culture platforms have advantages over traditional static cell culture systems. For example, Kirkstall (Rotherham, England) developed the 'Quasi Vivo system' aimed at the replication of the *in vivo*-like fluidic micro-environment by integrating a peristaltic pump and Transwell-based cell culture chamber. Additionally, SYNIVIVO (Huntsville, USA) also developed a 'SynBBB 3D Blood Brain Barrier Model' mimicking cellular morphology, interactions, and fluidic characteristics. This system contains a neural tissue compartment (basolateral chamber) in the center and vascular channel (apical chamber) separated by a porous barrier in a circular shape. The SynBBB System can enable the precise control of the hemodynamic shear stress and real-time visualization. These models reflect the demand for more physiologically relevant BBB models.

Overall, when ECs are exposed to shear stress and cocultured with other cell types, a higher TEER value and lower vascular permeability are observed than those in the Transwell model. Although these platforms are regarded as improved BBB models, they do not completely replicate the complex 3D geometries *in vivo*.

4.3. Spheroid-based BBB models

Cells comprising human organs directly or indirectly interact with the surrounding cells located in close proximity. Therefore, spheroid models have been developed to simulate physiological conditions *in vivo* in terms of complex multicellular interactions in a 3D structure. For example, tumor spheroid models, which are the most common platform applied in cancer research, have been widely used for drug development and fundamental studies of carcinogenesis and metastasis. Using a similar approach, BBB spheroid models are a promising platform for drug screening with high throughput, low complexity, and high accessibility (Fig. 6c).

Urlich et al. [187] first developed a multicellular BBB spheroid model using the 3D hanging-drop method and revealed the functional roles of pericytes and astrocytes in the maintenance of BBB integrity (Fig. 8a). A mixed cell suspension of human primary brain endothelial cells, human primary pericytes, and human primary astrocytes spontaneously form spheroid structures resembling the *in vivo* environment. Brain endothelial cells cover the outside of the spheroid as a shell by directly contacting pericytes and astrocytes positioned in the core region. Self-assembled BBB spheroids express cell adhesion molecules at higher levels than cells in the Transwell system. Here, pericytes are implicated in the stable organization of the spheroids by interacting with endothelial cells and astrocytes. Using a different approach for spheroid formation, Cho et al. [189] introduced two types of human BBB spheroid models using primary or immortalized endothelial cells and applied them as platforms to screen brain-penetrating agents (Fig. 8b). These spheroid models express TJ proteins at high levels and display increased efflux pump/transporter activity. The spheroid models demonstrated greater potential as a practical platform for CNS research than the traditional Transwell model because these models replicate direct cell-cell interactions in a 3D environment with high throughput and versatility. Boutin et al. [188] isolated cortical tissues from rats or mice and generated spheroids by culturing the primary tissues on an agarose-coated plate (Fig. 8c). The endothelial cells spontaneously formed a capillary-like network and hollow lumen in the absence of exogenous factors or protein-rich ECM. Their primary cell-derived BBB spheroid model features an *in vivo*-like cell density, diverse neural cell types, abundant basement membrane proteins, and brain-like stiffness, indicating good relevance to *in vivo* brain tissues. Nzou et al. [190] constructed human cortical spheroids composed of six cell types, including brain endothelial cells, pericytes, astrocytes, microglia, oligodendrocytes, and neurons, and applied them as a neurotoxicity

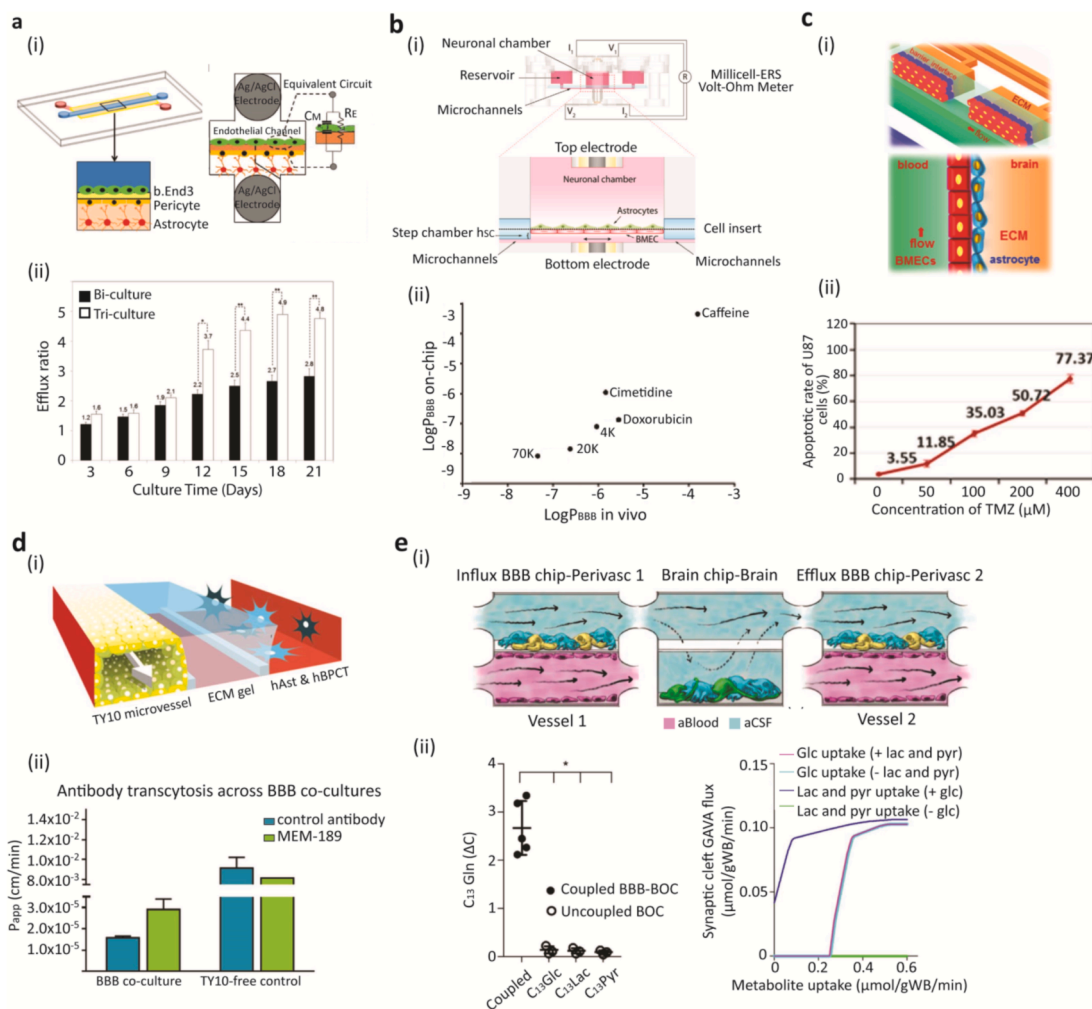


Fig. 7. Porous membrane-based 2D microfluidic BBB models. In these models, endothelial cells are seeded on the porous membrane, while other cell types are cultured on the opposite side or in the bottom chamber. To apply fluidic shear stress to the endothelial cells, the pump is connected to the vascular channel. In addition, the electrode can be integrated into the device to measure TEER. (a) The main components of the BBB (endothelial cells, pericytes, and astrocytes) are cocultured and the highest TEER value is verified in the triple culture group. Reprinted with permission from Wang et al. [183]. (b) Human iPSCs are differentiated into BMECs and then cocultured with astrocytes in the device. Although only two kinds of cells were cultured on the 2D platform, a significantly higher TEER value was observed, similar to the value observed *in vivo*. Reprinted with permission from Wang et al. [182]. (c) The tumor-cultured BBB model was applied to screen drug efficacy. TMZ, an anti-brain tumor drug, triggered the apoptosis of U87 cells cultured on a chip. Reprinted with permission from Xu et al. [178]. (d) When the antibody was infused into the microvessel channel, the antibody was transported to the ECM gel by transcytosis. This platform recapitulated not only the physical barrier property (permeability) but also selective transport (receptor-mediated transcytosis). Reprinted with permission from Wevers et al. [179]. (e) The perivascular part was linked to the neuronal part to assess metabolism in the brain. Fluidic coupling induced a change in metabolite production. Reprinted with permission from Maoz et al. [185].

model (Fig. 8d). The authors induced Parkinson's disease-associated dopaminergic neuron dysfunction and death by treating the cortical spheroids with 1-methyl-4-phenyl-1,2,3,6-tetrahydropyridine (MPTP). MPTP is known to pass through the BBB and produce the gliotoxic metabolite MPP⁺. In the BBB-positive spheroid model, MPTP reduces ATP production and cell death.

Although spheroid models recapitulate a greater number of *in vivo*-like characteristics, such as cell–cell and cell–ECM interactions, in a 3D microenvironment than the Transwell system, discrepancies between *in vivo* and *in vitro* observations remain due to the lack of intravascular fluid flow.

4.4. Hydrogel-laden 3D culture-based BBB models

In the brain, multiple cell types, including neurons, astrocytes, microglia, and oligodendrocytes, reside in the 3D microenvironment. These glial and neural cells have different phenotypes from those of cells cultured in conventional 2D plastic dishes. For example, 3D-

cultured astrocytes are less reactive (in the resting state) and display a complex and highly branched morphology, suggesting the suitability of the 3D environment to induce more *in vivo*-like phenotypes and functional characteristics of brain cells [43]. Actually, many studies have focused on culturing cells in the geometrically confined 3D hydrogel scaffold with particular emphasis on interactions among cells. Furthermore, hydrogels endow the system with brain tissue-like mechanical properties, such as a low stiffness and viscoelasticity [206,207]. Therefore, this hydrogel-laden 3D cell culture platform represents a physiologically relevant microenvironment for cells and is expected to provide new opportunities for fundamental studies and industrial applications of the BBB model.

Two approaches have been used to fabricate the microvasculature in a 3D hydrogel: bottom-up and top-down approaches (Fig. 6d). The bottom-up approach is based on the physiological processes of vasculogenesis and angiogenesis. Endothelial cells spontaneously form a complex and perfusable vascular network within the 3D gel and mimic the complexity of the native vasculature in terms of the *in vivo* diameter,

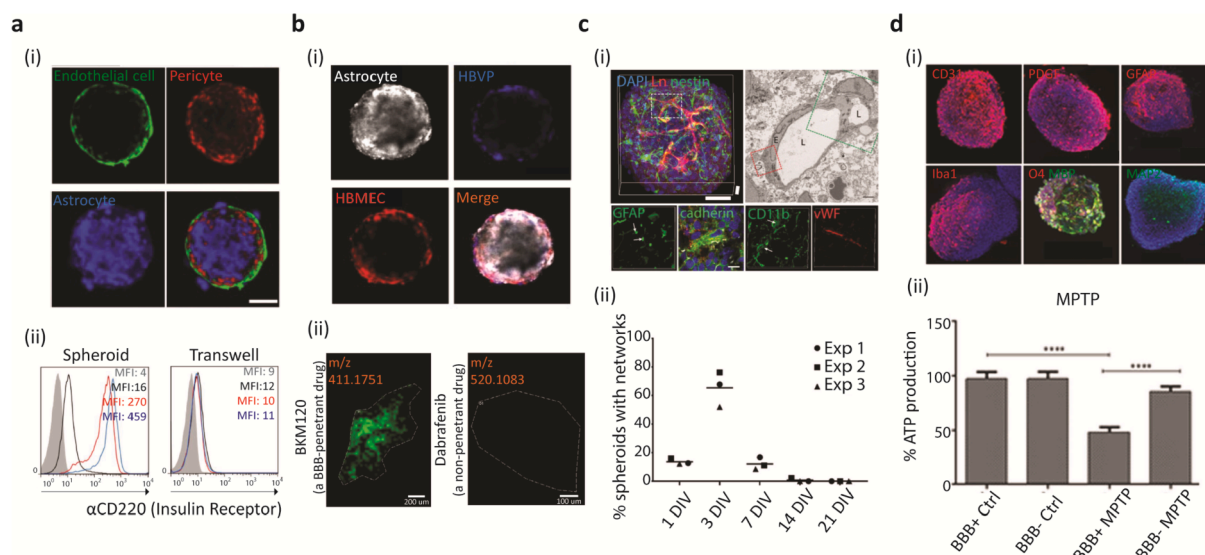


Fig. 8. Spheroid-based BBB models. In the BBB spheroid model, endothelial cells cover the outer surface of the spheroid and directly contact pericytes and astrocytes in the core. The presence of these three types of cells in spheroids is verified by labeling with a fluorescent tracker or staining with antibodies against specific markers. (a) The endothelial cells in the spheroid express the receptor at higher levels than those in cells cultured in the Transwell. Reprinted with permission from Urlich et al. [187]. (b) Additionally, when a BBB-penetrating drug was added to the spheroid, its transport was confirmed by capturing MALDI-MSI ion images. Reprinted with permission from Cho et al. [189]. (c) For organizing multicellular spheroids with *in vivo*-like cell types and densities, cortical cells are dissociated from the brain and then cultured on an agarose-coated substrate. Endothelial cells within the cortical cell suspension assemble into capillary-like structures and a basement membrane is also synthesized. In addition, the multicellular structure is verified by staining for markers of neuronal progenitor cells (nestin), astrocytes (GFAP), endothelial cells (cadherin), and microglia (CD11b). Reprinted with permission from Boutin et al. [188]. (d) The human cortical spheroid consists of six cell types (endothelial cells, pericytes, astrocytes, microglia, oligodendrocytes, and neurons). Following exposure to MPTP, the MPTP metabolite reduces ATP production in the spheroid. Reprinted with permission from Nzou et al. [190].

growth dynamics, and marker expression [193,195,208]. These self-assembly-based models are valuable tools for studies of various processes, such as cancer metastasis and angiogenesis. In a well-known bottom-up approach, the formation of a vascular network is induced by seeding endothelial cells in a 3D fibrin gel. Fibrin plays an essential role in angiogenesis during the wound healing process [209]. In the fibrin gel, endothelial cells self-organize into a vascular structure with a hollow lumen in the presence of stromal cells, such as fibroblasts [210–212]. Some studies have proposed roles for the chemokine gradient and interstitial flow in promoting angiogenic sprouting [213,214].

An improved BBB model consisting of a self-organized vascular network cocultured with astrocytes and neurons was developed (Fig. 9a) [193]. In this platform, the fibrin hydrogel is confined between an array of microposts, and endothelial cells are embedded in the fibrin hydrogel. Then, the astrocytes and neurons are attached to the sidewall of the fibrin gel. Interestingly, the contact of the angiogenic sprouting tip with astrocytes inhibited the further migration and invasion of the leader cell. The presence of astrocytes enhanced the barrier function and induced low vascular permeability. Recently, an integrated model of angiogenesis and neurogenesis has been reported (Fig. 9b). Uwamori et al. [195] constructed a neurovascular tissue by the tri-culture of BMECs with neural stem cells and mesenchymal stem cells in the hydrogel. Neural stem cells differentiate into neurons and extend neurites within the vascularized hydrogel. Recently, Campisi et al. [191] cocultured human iPSC-ECs, human brain pericytes, and astrocytes within the 3D fibrin gel (Fig. 9c). In the tri-culture model, the iPSC-ECs spontaneously organized into a microvascular network with high geometrical similarity to capillaries *in vivo* and low permeability (8.9×10^{-8} cm/s and 2.2×10^{-7} cm/s for 10 kDa and 40 kDa FITC-dextran).

In the top-down approach, the microvasculature is formed by attaching endothelial cells to the luminal surface of the preformed hydrogel channel. This approach allows the precise control of the vascular dimensions and therefore a uniform flow pattern can be reproduced

over the course of repeated experiments. Three types of technologies have been used to generate artificial lumen structures in bulk hydrogel: (i) the viscous fingering method, (ii) removal of the templates, such as microneedles, after gelation, and (iii) a patterned microvasculature. Herland et al. [194] prepared a hollow lumen using the viscous fingering method. As the culture medium flows through the partially gelled collagen, a hollow lumen is formed in the bulk hydrogel. Astrocytes or pericytes are premixed with collagen, and endothelial cells are attached to the luminal surface of the collagen channel after gelation (Fig. 9d). The authors identified the individual contributions of astrocytes and pericytes in response to neuroinflammatory stimulation. When the engineered endothelium was stimulated with TNF- α , the coculture system released greater amounts of cytokines (G-CSF, IL-6, and IL-8) than cells cultured in Transwells. BBB chips have potential applications for the independent assay of multicellular interactions, which is not possible *in vivo*.

Partyka et al. [196] reported the effects of blood flow-induced mechanical stimuli on the barrier function and waste transport (Fig. 9e). The microchannel structure was formed by removing microneedles from the gelatinized composite hydrogels composed of collagen type I, hyaluronan, and Matrigel. The authors replicated the *in vivo* environment by coculturing immortalized human cerebral endothelial cells with astrocytes under pulsatile flow. As shown in previous studies, mechanical stimulation increases the localization of TJs along the lateral cell membrane and decreases transendothelial permeability [172]. A significant finding of this study is that the mechanical environment in the cerebral circulatory system also affects waste transport. Pulsatile flow induces cyclic wall strain in the endothelial channel and moves particles along the apical face in the reverse direction to the applied flow. Adriani et al. [192] engineered a 3D neurovascular chip by coculturing cerebral microvascular endothelial cells with cortical neurons and astrocytes within separate channels defined by trapezoidal microposts (Fig. 9f). Endothelial cells closely interact with neurons and astrocytes as they are located adjacent to the neural/glial mixed hydrogel channel. The authors provided evidence for the morphological

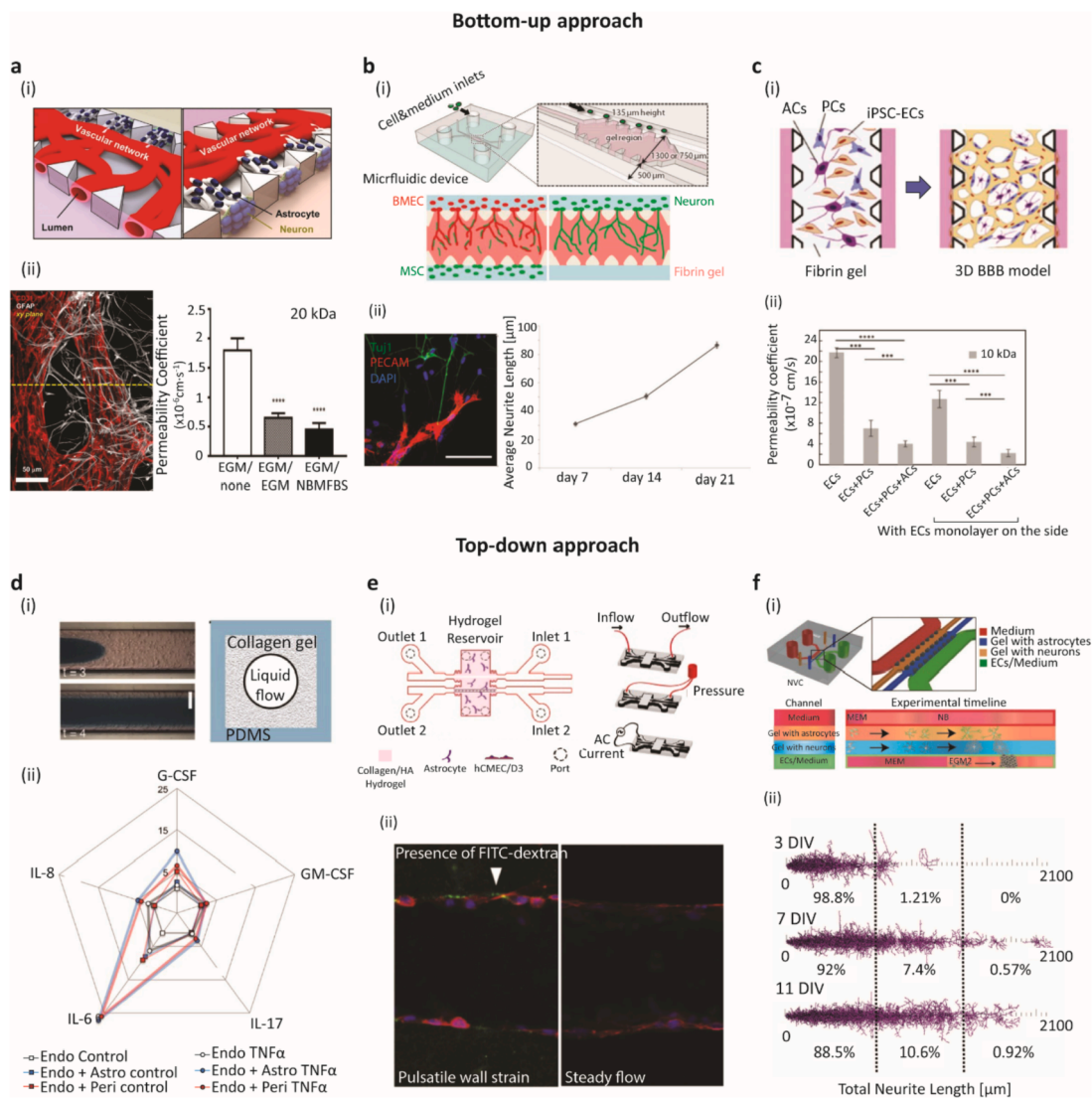


Fig. 9. Hydrogel-laden 3D microfluidic BBB models. Two approaches have been used to form the microvasculature in the bulk hydrogel: bottom-up and top-down approaches. The bottom-up approach is based on the physiological process in which endothelial cells spontaneously proliferate and organize within the hydrogel, forming a perfusable vascular network. (a) After the formation of the vascular network, astrocytes/neurons are seeded on the other side of the endothelial cell-seeded channel to induce low permeability. Reprinted with permission from Bang et al. [193]. (b) Similarly, the endothelial cells form a vascular structure until they contact neurons. Reprinted with permission from Uwamori et al. [195]. (c) Human iPSC-derived ECs also form capillary-like structures, and coculture of the vascular network with pericytes and astrocytes produces a permeability coefficient similar to *in vivo* conditions. In the top-down approach, the microvasculature is fabricated by attaching endothelial cells to predefined microchannels. Reprinted with permission from Campisi et al. [191]. (d) When the medium was injected into the semigelled hydrogel, the channel was formed due to the difference in viscosity. The channel dimension can be controlled, depending on the differences between the inlet and outlet pressures. The embedded pericytes or astrocytes directly interact with the microvasculature on the abluminal side. Reprinted with permission from Herland et al. [194]. (e) The microneedle was injected into the sol state hydrogel, which contains other cell types, and it was removed after gelation was complete. The channel dimension depends on the microneedle size. Reprinted with permission from Partyka et al. [196]. (f) A patterned hydrogel can be applied in the BBB model. The chip contains separate channels defined by trapezoidal microposts. The cell-embedded gel is separately injected into the channels and endothelial cells are seeded in one empty channel. Reprinted with permission from Adriani et al. [192].

similarity of endothelial cells in terms of the sprouting branches in 3D matrices and functional characteristics of endothelial barrier. The lowest endothelial permeability and increased neurite length and number observed in the tri-culture model (brain endothelial cells, pericytes, and astrocytes) confirmed the importance of multicellular interactions in the expression of functional phenotypes *in vitro*. The barrier function of the engineered BBB was evaluated by introducing monosodium glutamate, a neurotransmitter, and observing calcium oscillations in hydrogel-embedded cells upon exposure to potassium chloride (KCl). This analysis confirmed that the well-organized endothelium contributes to the maintenance of brain homeostasis by restricting the passage of neural activators from the vascular network to the neural tissue.

Both bottom-up and top-down approaches have strengths and limitations as an *in vitro* model. For example, the bottom-up approach mimics the *in vivo* dynamics of angio- and vasculogenesis to a greater extent, but the dynamic morphological changes in the vascular structure limit the control of the vascular geometry, such as the vessel diameter, length, and flow pattern. In contrast, the advantages of top-down technologies include the fabrication and preservation of a predefined vascular geometry, but small-scale channels mimicking capillaries (with a diameter of less than 50 μm) are difficult to fabricate. In the microcirculation system, the capillary has a diameter ranging from 7 μm to 10 μm and the intervascular distance is approximately 40 μm [5,19,215]. Therefore, an innovative approach that overcomes the limitations of bottom-up and top-down approaches must be developed.

5. Quantification of *in vitro* barrier function: trans-endothelial electrical resistance (TEER)

A characteristic feature of endothelial cells is TJ formation. Since the presence of an intact barrier is crucial for reliable *in vitro* experiments, techniques have been developed to quantify barrier integrity. For example, TEER measurement estimates the electrical, ohmic resistance of the cell layer [216]. Based on Ohm's law, the electrical resistance of a cellular monolayer, measured in ohms is obtained as a quantitative measure of barrier integrity. For electrical measurements, two electrodes are used. In the case of Transwell assays, one electrode is placed in the upper compartment and the other is located in the lower compartment; the electrodes are therefore separated by the cellular monolayer. The ohmic resistance can be determined by applying a direct current (DC) to the electrodes and measuring the resulting current. The ohmic resistance is calculated based on Ohm's law as the ratio of the voltage to the current. However, DC currents may damage both the cells and the electrodes. To overcome this issue, an alternating current (AC) can be utilized [200].

In terms of the electrode number, there are usually two ways to measure TEER: two-wire and four-wire TEER measurement systems. In two-wire TEER measurements, the BBB chip was connected to an HP4194A impedance/gain phase analyzer. Impedance spectra were recorded using AC with an amplitude of 10 mV ranging from 1 Hz to 3 MHz over the two Pt electrodes. The average of this model is $28.2 \pm 1.3 \Omega \text{ cm}^2$ in the Transwell and $36.9 \pm 0.9 \Omega \text{ cm}^2$ in the BBB chip. Furthermore, after shear stress was applied to the chip, the TEER value increased to $120 \Omega \text{ cm}^2$ [217].

Another automated multi-well TEER measurement chamber has been developed to automatically measure the time course of TEER under ordinary cell culture conditions (37 °C, 5% or 10% CO₂). In each well, the cell layer is sandwiched between the two electrodes and is exposed to a homogeneous electric field along the entire surface of the cell layer so that accurate transepithelial impedance readings can be recorded. The dipping electrodes are individually addressable by the software. The device sequentially reads the electrical AC impedance of each filter insert at a preset number of frequencies in between 1 and 105 Hz. The average of this model is $382.7 \Omega \text{ cm}^2$ [218].

The computer-controlled TEER measurement model is also available. In this model, cells are cultured directly on thin gold-film electrodes and electrochemical impedance is measured to study passive electrical properties. Based on impedance spectra (10–2 × 10⁶ Hz) of confluent cell monolayers, electrical characteristics can be modeled by simple resistors and capacitors in parallel. Under control conditions, the overall resistance of confluent cell monolayers was $3.6 \pm 0.6 \Omega \text{ cm}^2$ [219].

Impedance spectroscopy when combined with a fitting algorithm provides a more accurate representation of TEER values than traditional DC/single frequency AC measurement systems [200]. This system measures resistance across endothelial barriers by embedding Ag/AgCl electrodes within a two-layer PDMS microfluidic chip where an upper and a lower channel are separated by a semiporous membrane. This system allows the reliable real-time measurement of TEER. Impedance spectra were taken using an Autolab potentiostat/galvanostat (EcoChemie). AC of amplitude 0.1 V was passed between the two embedded Ag/AgCl electrodes in the frequency range from 10 Hz to 1.00 MHz. Endothelial barrier resistance was 150–200 $\Omega \text{ cm}^2$ [220].

In another example, measurements are obtained across a cell layer immobilized on a microfluidic device enabling interactions between the cell layer and a flowing stream of red blood cells. Applying a bipolar pulsed square wave potential across a monolayer of bovine pulmonary artery endothelial cells, the current response was measured and integrated. After cell seeding on the device, there was a decrease in TEER from $40.9 \pm 2.9 \Omega \text{ cm}^2$ to $259.1 \pm 27.4 \Omega \text{ cm}^2$ [221].

TEER in organs-on-chips can be directly determined with four electrodes and six measurements. This method is suitable for arbitrary

chips with two channels in which two electrodes can be inserted, while still being compatible with the simple measurement setup used for conventional 2-electrode TEER measurements. The four-electrode method enables the direct isolation of the membrane resistance, regardless of variation in the system. An average TEER of $22 \Omega \text{ cm}^2$ was obtained (across 4 chips) [227].

Existing systems for measuring TEER are not suitable for integration with body-on-a-chip systems due to the small cell culture area, which is not easily accessible for electrode positioning close to the cell culture area. Furthermore, the variation between measurements when electrodes are not firmly secured in the same position is also a problem [200].

6. Perspectives and conclusions

The barrier function of the BBB is indispensable for regulating the transport of molecules between the cerebral circulatory system and neural tissue. The BBB is highly impermeable to a variety of molecules and particles but allows the selective influx and outflux of gases, nutrients, proteins, and metabolic waste in the CNS. BBB breakdown facilitates the entry of cytotoxic materials, leading to the development of neurological dysfunction, synapse loss, and neuronal injury. This phenomenon is the hallmark of many CNS disorders, such as Alzheimer's disease, Parkinson's disease, Huntington's disease, acute and chronic cerebrovascular diseases, and inflammatory diseases [11,12]. Despite efforts to elucidate the molecular mechanisms underlying CNS diseases, studies are limited by the complex interplay among *in vivo* components, such as the immune response and surrounding stromal reaction. This complexity hampers the abilities to decouple the particular functions of pathways associated with and responses caused by specific elements. Among cell-based *in vitro* platforms, the 3D-based microfluidic model replicates *in vivo* structures and complexity in a timely and cost-effective manner. Although these models are promising for biomedical applications as a complementary approach, various challenges need to be overcome before they are used as a reliable and robust platform.

One challenge in the development of BBB models is the availability of reliable and abundant cell sources that maintain BBB-specific functions *in vitro*. Generally, most BBB models are established with primary or immortalized cells of animal or human origin. The immortalized cells from animals (rat EC lines: RBE4, mouse EC lines: b. END3, b. END5 and MBEC4) and humans (EC lines: BB19, HCEC, HBEC-5i, NKIM-6, HBMEC-3, TY08 and HBMEC/ciβ) have the advantages of high reproducibility compared to primary cells [176,222]. However, they possess few BBB-specific properties, such as a low TEER of less than $150 \Omega \text{ cm}^2$ and high permeability, compared with physiological values. In particular, genetic characteristics and pathological mechanisms differ between human cells and other animal cells. These structural and biochemical differences in nonhuman species can lead to inaccurate predictions of drug efficacy.

Therefore, in recent studies, human stem cell-based BBB models have been established as an alternative and powerful tool [223]. Human induced pluripotent stem cells or progenitor cells are available as an effective cell source without the need for isolating cells from the human brain, and show BBB functions when they are differentiated into brain cells using the proper protocol. These models have the advantages of high reproducibility and stability compared to primary cells, which only maintain their phenotype for a limited number of passages. In 2014, Lippmann et al. [175] differentiated human pluripotent stem cells into brain microvascular endothelial cells (BMECs) and then co-cultured them on a Transwell with human pericytes, astrocytes, and neurons derived from human neural progenitor cells (NPCs). The authors observed enhanced barrier properties (TEER values greater than $5000 \Omega \text{ cm}^2$, upregulation of TJ-related proteins and increased efflux activity) by treating BMECs with retinoic acid, which is secreted by radial glia. Additionally, Appelt-Menzel et al. [176] differentiated human induced pluripotent stem cells into endothelial cells and

astrocytes and developed the quadruple culture model by coculturing various BBB cell types (hiPS-ECs, hiPS-neural stem cells, astrocytes, and pericytes) in Transwells. Differentiated cells (astrocytes and neurons) were characterized by staining for cell-specific markers. The *in vivo*-like TEER value (up to 2500 Ω cm²) and upregulation of BBB-related genes were achieved in the quadruple culture model, suggesting that stem cells have the potential to be used as an alternative cell source to model the BBB. This improved model can be applied to the development of a personalized disease model composed of patient-derived cells. Recently, many researchers have focused on replicating *in vitro* BBB models using stem cell-derived BBB cells for applications in personalized medicine [131]. Individual patients with the same disease exhibit heterogeneous responses to drugs due to underlying genetic variation. From this perspective, the *in vitro* BBB models composed of patient-derived cells are expected to be used as a patient-specific avatar for testing drug efficacy and optimizing drug compositions.

Another limitation of current *in vitro* BBB models is the inability to completely replicate the brain microenvironment *in vivo*, including the multicellular structure and ECM composition. Most studies employ the coculture of limited types of cells (e.g., not including microglia, oligodendrocytes, and neural stem cells) owing to the lack of advanced coculture techniques. Microglia, which are immune cells within the CNS, are associated with cerebral angiogenesis and neuroinflammation. These cells exhibit cross-talk with endothelial tip cells during angiogenic sprouting [224]. In addition, oligodendrocyte precursor cells also promote BBB integrity by secreting TGF- β 1 and increasing the levels of TJ proteins [225]. Based on these results, microglia and oligodendrocytes are required for ensuring BBB integrity and accurately simulating the physiological and pathological phenomena observed in the BBB.

Compared with other tissues, brain tissues express low levels of fibrous proteins, such as collagen, and high levels of glycosaminoglycans, proteoglycans, and hyaluronan. Among fibrous proteins, collagen type IV and laminin are mainly located in the basement membrane of cerebral endothelial cells, rather than the neural tissue [156,157]. Diverse types of ECMs are involved in neuronal development, function, and degeneration, suggesting that a combination of ECM components with important functions *in vivo* is essential to precisely replicate physiological cell behaviors or responses. However, most current *in vitro* BBB models are based on collagen type I or Matrigel (with high collagen type IV and laminin contents) owing to their accessibility and affordability. According to Placone et al. [226], astrocytes cultured in an optimized gel composed of collagen, hyaluronic acid, and Matrigel exhibit a star-shaped morphology and maintain a quiescent state with a low level of GFAP expression. Thus, the scaffold material is a key element for obtaining physiological morphologies and functions using *in vitro* models.

In summary, we reviewed recent advances in the development of *in vitro* BBB models. Several *in vitro* models, ranging from Transwell systems to hydrogel-laden 3D microfluidic models, have been developed to recapitulate the physiology of the BBB using engineering techniques. Despite many attempts to simulate the BBB characteristics *in vivo* by integrating the microenvironment (3D, ECM, and fluidic shear stress) into platforms, further improvements are needed in terms of cell sources, biomaterials, and external stimuli. Reliable and more physiologically relevant *in vitro* BBB models are anticipated and are expected to revolutionize the fundamental biomedical studies of disease mechanisms as well as drug discovery and testing.

Declaration of competing interest

The authors have no competing financial interests to declare.

Acknowledgements

This work was supported by a grant from the National Research

Foundation of Korea (NRF) funded by the Korean Government (MSIT) (grant no. 2018R1A2A3075013), the Brain Research Program through the National Research Foundation of Korea (NRF) funded by the Ministry of Science and ICT (NRF-2016M3C7A1913845), the Technology Innovation Program (10067787) funded by the Ministry of Trade, Industry & Energy (MOTIE, Korea), the KIST Institutional Program (2E29200 and 2V07460), and a grant from the National Research Foundation of Korea (NRF) funded by the Ministry of Science and ICT (2017M3A7B4049850). This work was supported by the KU-KIST School Project.

References

- [1] I. Wilhelm, I.A. Krizbai, *In vitro* models of the blood-brain barrier for the study of drug delivery to the brain, *Mol. Pharm.* 11 (7) (2014) 1949–1963.
- [2] W.M. Pardridge, The blood-brain barrier: bottleneck in brain drug development, *NeuroRx* 2 (1) (2005) 3–14.
- [3] W.M. Pardridge, Drug transport across the blood-brain barrier, *J. Cereb. Blood Flow Metab.* 32 (11) (2012) 1959–1972.
- [4] B.V. Zlokovic, Neurovascular pathways to neurodegeneration in Alzheimer's disease and other disorders, *Nat. Rev. Neurosci.* 12 (12) (2011) 723–738.
- [5] C. Nicholson, Diffusion and related transport mechanisms in brain tissue, *Rep. Prog. Phys.* 64 (7) (2001) 815.
- [6] B. Obermeier, R. Daneman, R.M. Ransohoff, Development, maintenance and disruption of the blood-brain barrier, *Nat. Med.* 19 (12) (2013) 1584–1596.
- [7] C.S. von Bartheld, J. Bahney, S. Herculano-Houzel, The search for true numbers of neurons and glial cells in the human brain: a review of 150 years of cell counting, *J. Comp. Neurol.* 524 (18) (2016) 3865–3895.
- [8] K.E. Schlageter, P. Molnar, G.D. Lapin, D.R. Groothuis, Microvessel organization and structure in experimental brain tumors: microvessel populations with distinctive structural and functional properties, *Microvasc. Res.* 58 (3) (1999) 312–328.
- [9] G. Perea, M. Sur, A. Araque, Neuron-glia networks: integral gear of brain function, *Front. Cell. Neurosci.* 8 (2014) 378.
- [10] H. Girouard, C. Iadecola, Neurovascular coupling in the normal brain and in hypertension, stroke, and Alzheimer disease, *J. Appl. Physiol.* 100 (1) (2006) 328–335.
- [11] Y. Yang, G.A. Rosenberg, Blood-brain barrier breakdown in acute and chronic cerebrovascular disease, *Stroke* 42 (11) (2011) 3323–3328.
- [12] M.D. Sweeney, A.P. Sagare, B.V. Zlokovic, Blood-brain barrier breakdown in Alzheimer disease and other neurodegenerative disorders, *Nat. Rev. Neurol.* 14 (3) (2018) 133–150.
- [13] I. Wilhelm, C. Fazakas, I.A. Krizbai, *In vitro* models of the blood-brain barrier, *Acta Neurobiol. Exp.* 71 (1) (2011) 113–128.
- [14] S. Festing, R. Wilkinson, The ethics of animal research: talking point on the use of animals in scientific research, *EMBO Rep.* 8 (6) (2007) 526–530.
- [15] T. Hartung, Thoughts on limitations of animal models, *Park. Relat. Disord.* 14 (Suppl 2) (2008) S81–S83.
- [16] J. Potashkin, S. Blume, N. Runkle, Limitations of animal models of Parkinson's disease, *Parkinson's Dis.* 2011 (2011) 658083.
- [17] P.K. Pandey, A.K. Sharma, U. Gupta, Blood brain barrier: an overview on strategies in drug delivery, realistic *in vitro* modeling and *in vivo* live tracking, *Tissue Barriers* 4 (1) (2016) e1129476.
- [18] P. Naik, L. Cucullo, *In vitro* blood-brain barrier models: current and perspective technologies, *J. Pharm. Sci.* 101 (4) (2012) 1337–1354.
- [19] A. Wolff, M. Antfolk, B. Brodin, M. Tenje, *In vitro* blood-brain barrier models—an overview of established models and new microfluidic approaches, *J. Pharm. Sci.* 104 (9) (2015) 2727–2746.
- [20] M.I. Bogorad, J. DeStefano, J. Karlsson, A.D. Wong, S. Gerecht, P.C. Searson, Review: *in vitro* microvessel models, *Lab Chip* 15 (22) (2015) 4242–4255.
- [21] B. Prabhakarandian, M.C. Shen, J.B. Nichols, I.R. Mills, M. Sidoryk-Wegrzynowicz, M. Aschner, K. Pant, SyM-BBB: a microfluidic blood brain barrier model, *Lab Chip* 13 (6) (2013) 1093–1101.
- [22] R.A. Hawkins, R.L. O'kane, I.A. Simpson, J.R. Vina, Structure of the blood-brain barrier and its role in the transport of amino acids, *J. Nutr.* 136 (1) (2006) 218S–226S.
- [23] W. Risau, Development and differentiation of endothelium, *Kidney Int.* 54 (1998) S3–S6.
- [24] R.M. Linville, J.G. DeStefano, M.B. Sklar, Z. Xu, A.M. Farrell, M.I. Bogorad, C. Chu, P. Walczak, L. Cheng, V. Mahairaki, K.A. Whartenby, P.A. Calabresi, P.C. Searson, Human iPSC-derived blood-brain barrier microvessels: validation of barrier function and endothelial cell behavior, *Biomaterials* 190–191 (2019) 24–37.
- [25] F. Joó, Endothelial cells of the brain and other organ systems: some similarities and differences, *Prog. Neurobiol.* 48 (3) (1996) 255–273.
- [26] J.F. Deeken, W. Loscher, The blood-brain barrier and cancer: transporters, treatment, and Trojan horses, *Clin. Cancer Res.* 13 (6) (2007) 1663–1674.
- [27] F.E. Arthur, R.R. Shivers, P.D. Bowman, Astrocyte-mediated induction of tight junctions in brain capillary endothelium: an efficient *in vitro* model, *Brain Res.* 433 (1) (1987) 155–159.
- [28] O.C. Colgan, N.T. Collins, G. Ferguson, R.P. Murphy, Y.A. Birney, P.A. Cahill, P.M. Cummins, Influence of basolateral condition on the regulation of brain microvascular endothelial tight junction properties and barrier function, *Brain Res.*

- 1193 (2008) 84–92.
- [29] S. Dohgu, F. Takata, A. Yamauchi, S. Nakagawa, T. Egawa, M. Naito, T. Tsuruo, Y. Sawada, M. Niwa, Y. Kataoka, Brain pericytes contribute to the induction and up-regulation of blood–brain barrier functions through transforming growth factor- β production, *Brain Res.* 1038 (2) (2005) 208–215.
- [30] S. Hori, S. Ohtsuki, K.I. Hosoya, E. Nakashima, T. Terasaki, A pericyte-derived angiopoietin-1 multimeric complex induces occludin gene expression in brain capillary endothelial cells through Tie-2 activation *in vitro*, *J. Neurochem.* 89 (2) (2004) 503–513.
- [31] J. Neuhaus, W. Risau, H. Wolburg, Induction of blood–brain barrier characteristics in bovine brain endothelial cells by rat astroglial cells in transfilter coculture, *Ann. N. Y. Acad. Sci.* 633 (1) (1991) 578–580.
- [32] J. Barar, M.A. Rafi, M.M. Pourseif, Y. Omid, Blood–brain barrier transport machineries and targeted therapy of brain diseases, *Bioimpacts* 6 (4) (2016) 225–248.
- [33] A.D. Wong, M. Ye, A.F. Levy, J.D. Rothstein, D.E. Bergles, P.C. Searson, The blood–brain barrier: an engineering perspective, *Front. Neuroeng.* 6 (2013) 7.
- [34] S.M. Stamatovic, R.F. Keep, A.V. Andjelkovic, Brain endothelial cell–cell junctions: how to “open” the blood brain barrier, *Curr. Neuropharmacol.* 6 (3) (2008) 179–192.
- [35] S. Tietz, B. Engelhardt, Brain barriers: crosstalk between complex tight junctions and adherens junctions, *J. Cell Biol.* 209 (4) (2015) 493–506.
- [36] A.-C. Luissint, C. Artus, F. Glacial, K. Ganeshamoorthy, P.-O. Couraud, Tight junctions at the blood brain barrier: physiological architecture and disease-associated dysregulation, *Fluids Barriers CNS* 9 (1) (2012) 23.
- [37] W.Y. Liu, Z.B. Wang, L.C. Zhang, X. Wei, L. Li, Tight junction in blood–brain barrier: an overview of structure, regulation, and regulator substances, *CNS Neurosci. Therapy* 18 (8) (2012) 609–615.
- [38] A.S. Fanning, L.L. Mitic, J.M. Anderson, Transmembrane proteins in the tight junction barrier, *J. Am. Soc. Nephrol.* 10 (6) (1999) 1337–1345.
- [39] H. Chiba, M. Osanai, M. Murata, T. Kojima, N. Sawada, Transmembrane proteins of tight junctions, *Biochim. Biophys. Acta* 1778 (3) (2008) 588–600.
- [40] M.S. Balda, K. Matter, Transmembrane proteins of tight junctions, *Semin. Cell Dev. Biol.* 11 (4) (2000) 281–289.
- [41] N. Weiss, F. Miller, S. Cazaubon, P.O. Couraud, The blood–brain barrier in brain homeostasis and neurological diseases, *Biochim. Biophys. Acta* 1788 (4) (2009) 842–857.
- [42] T. Hirase, J.M. Staddon, M. Saitou, Y. Ando-Akatsuka, M. Itoh, M. Furuse, K. Fujimoto, S. Tsukita, L.L. Rubin, Occludin as a possible determinant of tight junction permeability in endothelial cells, *J. Cell Sci.* 110 (14) (1997) 1603–1613.
- [43] J. Woo, S.K. Im, H. Chun, S.Y. Jung, S.J. Oh, N. Choi, C.J. Lee, E.M. Hur, Functional characterization of resting and adenovirus-induced reactive astrocytes in three-dimensional culture, *Exp. Neurobiol.* 26 (3) (2017) 158–167.
- [44] T. Nitta, M. Hata, S. Gotoh, Y. Seo, H. Sasaki, N. Hashimoto, M. Furuse, S. Tsukita, Size-selective loosening of the blood–brain barrier in claudin-5-deficient mice, *J. Cell Biol.* 161 (3) (2003) 653–660.
- [45] A.-C. Luissint, C. Federici, F. Guillonnet, F. Chrétien, L. Camoin, K. Ganeshamoorthy, P.-O. Couraud, Guanine nucleotide-binding protein Gai2: a new partner of claudin-5 that regulates tight junction integrity in human brain endothelial cells, *J. Cereb. Blood Flow Metab.* 32 (5) (2012) 860–873.
- [46] D. Yeung, J.L. Manias, D.J. Stewart, S. Nag, Decreased junctional adhesion molecule-A expression during blood–brain barrier breakdown, *Acta Neuropathol.* 115 (6) (2008) 635–642.
- [47] K.J. Mandell, C.A. Parkos, The JAM family of proteins, *Adv. Drug Deliv. Rev.* 57 (6) (2005) 857–867.
- [48] K. Umeda, T. Matsui, M. Nakayama, K. Furuse, H. Sasaki, M. Furuse, S. Tsukita, Establishment and characterization of cultured epithelial cells lacking expression of ZO-1, *J. Biol. Chem.* 279 (43) (2004) 44785–44794.
- [49] O. Tornavaca, M. Chia, N. Dufton, L.O. Almagro, D.E. Conway, A.M. Randi, M.A. Schwartz, K. Matter, M.S. Balda, ZO-1 controls endothelial adherens junctions, cell–cell tension, angiogenesis, and barrier formation, *J. Cell Biol.* 208 (6) (2015) 821–838.
- [50] T. Katsuno, K. Umeda, T. Matsui, M. Hata, A. Tamura, M. Itoh, K. Takeuchi, T. Fujimori, Y. Nabeshima, T. Noda, S. Tsukita, S. Tsukita, Deficiency of zonula occludens-1 causes embryonic lethal phenotype associated with defected yolk sac angiogenesis and apoptosis of embryonic cells, *Mol. Biol. Cell* 19 (6) (2008) 2465–2475.
- [51] J. Xu, P.J. Kausalya, D.C. Phua, S.M. Ali, Z. Hossain, W. Hunziker, Early embryonic lethality of mice lacking ZO-2, but Not ZO-3, reveals critical and nonredundant roles for individual zonula occludens proteins in mammalian development, *Mol. Cell Biol.* 28 (5) (2008) 1669–1678.
- [52] N.J. Abbott, A.A. Patabendige, D.E. Dolman, S.R. Yusof, D.J. Begley, Structure and function of the blood–brain barrier, *Neurobiol. Dis.* 37 (1) (2010) 13–25.
- [53] A. Taddei, C. Giampietro, A. Conti, F. Orsenigo, F. Breviario, V. Pirazzoli, M. Potente, C. Daly, S. Dimmeler, E. Dejuna, Endothelial adherens junctions control tight junctions by VE-cadherin-mediated upregulation of claudin-5, *Nat. Cell Biol.* 10 (8) (2008) 923–934.
- [54] W.A. Banks, Characteristics of compounds that cross the blood–brain barrier, *BMC Neurol.* 9 (Suppl 1) (2009) S3.
- [55] A.H. Schinkel, P-Glycoprotein, a gatekeeper in the blood–brain barrier, *Adv. Drug Deliv. Rev.* 36 (2–3) (1999) 179–194.
- [56] N.J. Yang, M.J. Hinner, Getting across the cell membrane: an overview for small molecules, peptides, and proteins, *Methods Mol. Biol.* 1266 (2015) 29–53.
- [57] Y. Serlin, I. Shelef, B. Knyazer, A. Friedman, *Anatomy and Physiology of the Blood–Brain Barrier*, Seminars in Cell & Developmental Biology, Elsevier, 2015, pp. 2–6.
- [58] Y. Kubo, S. Ohtsuki, Y. Uchida, T. Terasaki, Quantitative determination of luminal and abluminal membrane distributions of transporters in porcine brain capillaries by plasma membrane fractionation and quantitative targeted proteomics, *J. Pharm. Sci.* 104 (9) (2015) 3060–3068.
- [59] W. Löscher, H. Potschka, Blood–brain barrier active efflux transporters: ATP-binding cassette gene family, *NeuroRx* 2 (1) (2005) 86–98.
- [60] P. Ramakrishnan, The role of P-glycoprotein in the blood–brain barrier, *Einstein Q. J. Biol. Med.* 19 (1) (2003) 160–165.
- [61] U. Mayer, E. Wagenaar, J.H. Beijnen, J.W. Smit, D.K. Meijer, J. Asperen, P. Borst, A.H. Schinkel, Substantial excretion of digoxin via the intestinal mucosa and prevention of long-term digoxin accumulation in the brain by the mdrla P-glycoprotein, *Br. J. Pharmacol.* 119 (5) (1996) 1038–1044.
- [62] R.B. Kim, Drugs as P-glycoprotein substrates, inhibitors, and inducers, *Drug Metab. Rev.* 34 (1–2) (2002) 47–54.
- [63] J.M. Tarasoff-Conway, R.O. Carare, R.S. Osorio, L. Glodzik, T. Butler, E. Fieremans, L. Axel, H. Rusinek, C. Nicholson, B.V. Zlokovic, Clearance systems in the brain—implications for Alzheimer disease, *Nat. Rev. Neurol.* 11 (8) (2015) 457–470.
- [64] K.A. Nałecz, Solute carriers in the blood–brain barrier: safety in abundance, *Neurochem. Res.* 42 (3) (2017) 795–809.
- [65] R.A. Hawkins, R.L. O’kane, I.A. Simpson, J.R. Vina, Structure of the blood–brain barrier and its role in the transport of amino acids, *J. Nutr.* 136 (1) (2006) 218S–226S.
- [66] C. Nicholson, Diffusion and related transport mechanisms in brain tissue, *Rep. Prog. Phys.* 64 (7) (2001) 815.
- [67] M.S. McAllister, L. Krizanac-Bengez, F. Macchia, R.J. Naftalin, K.C. Pedley, M.R. Mayberg, M. Marroni, S. Leaman, K.A. Stanness, D. Janigro, Mechanisms of glucose transport at the blood–brain barrier: an *in vitro* study, *Brain Res.* 904 (1) (2001) 20–30.
- [68] S.G. Patching, Glucose transporters at the blood–brain barrier: function, regulation and gateways for drug delivery, *Mol. Neurobiol.* 54 (2) (2017) 1046–1077.
- [69] K. Shah, S. DeSilva, T. Abbruscato, The role of glucose transporters in brain disease: diabetes and Alzheimer’s disease, *Int. J. Mol. Sci.* 13 (10) (2012) 12629–12655.
- [70] E.A. Winkler, Y. Nishida, A.P. Sagare, S.V. Rege, R.D. Bell, D. Perlmutter, J.D. Sengillo, S. Hillman, P. Kong, A.R. Nelson, GLUT1 reductions exacerbate Alzheimer’s disease vasculo-neuronal dysfunction and degeneration, *Nat. Neurosci.* 18 (4) (2015) 521.
- [71] M.A. Kohli, S. Lucae, P.G. Saemann, M.V. Schmidt, A. Demirkan, K. Hek, D. Czamara, M. Alexander, D. Salyakina, S. Ripke, The neuronal transporter gene SLC6A15 confers risk to major depression, *Neuron* 70 (2) (2011) 252–265.
- [72] R.K. Upadhyay, Transendothelial transport and its role in therapeutics, *International scholarly research notices* (2014) 2014.
- [73] I. Sayeed, N. Turan, D.G. Stein, B. Wali, Vitamin D deficiency increases blood–brain barrier dysfunction after ischemic stroke in male rats, *Exp. Neurol.* 312 (2019) 63–71.
- [74] S. Ayloo, C. Gu, Transcytosis at the blood–brain barrier, *Curr. Opin. Neurobiol.* 57 (2019) 32–38.
- [75] A. Ben-Zvi, B. Lacoste, E. Kur, B.J. Andreone, Y. Mayshar, H. Yan, C. Gu, Mfsd2a is critical for the formation and function of the blood–brain barrier, *Nature* 509 (7501) (2014) 507.
- [76] R. Villaseñor, J. Lampe, M. Schwaninger, L. Collin, Intracellular transport and regulation of transcytosis across the blood–brain barrier, *Cell. Mol. Life Sci.* 76 (6) (2019) 1081–1092.
- [77] G.J. Doherty, H.T. McMahon, Mechanisms of endocytosis, *Annu. Rev. Biochem.* 78 (2009) 857–902.
- [78] S. Mayor, R.G. Parton, J.G. Donaldson, Clathrin-independent pathways of endocytosis, *Cold Spring Harb. Perspect. Biol.* 6 (6) (2014) a016758.
- [79] A.S. Haqqani, G. Thom, M. Burrell, C.E. Delaney, E. Brunette, E. Baumann, C. Sodja, A. Jezierski, C. Webster, D.B. Stanimirovic, Intracellular sorting and transcytosis of the rat transferrin receptor antibody OX26 across the blood–brain barrier *in vitro* is dependent on its binding affinity, *J. Neurochem.* 146 (6) (2018) 735–752.
- [80] R. Villaseñor, M. Schilling, J. Sundaresan, Y. Lutz, L. Collin, Sorting tubules regulate blood–brain barrier transcytosis, *Cell Rep.* 21 (11) (2017) 3256–3270.
- [81] A.R. Jones, E.V. Shusta, Blood–brain barrier transport of therapeutics via receptor-mediated, *Pharm. Res.* 24 (9) (2007) 1759–1771.
- [82] F. Hervé, N. Ghinea, J.-M. Scherrmann, CNS delivery via adsorptive transcytosis, *AAPS J.* 10 (3) (2008) 455–472.
- [83] S.B. Hladky, M.A. Barrand, Fluid and ion transfer across the blood–brain and blood–cerebrospinal fluid barriers; a comparative account of mechanisms and roles, *Fluids Barriers CNS* 13 (1) (2016) 19.
- [84] G.G. Somjen, Ion regulation in the brain: implications for pathophysiology, *The Neuroscientist* 8 (3) (2002) 254–267.
- [85] R. Llinas, The Role of Calcium in Neuronal Function, the Neurosciences, Fourth Study Program, 1979, pp. 555–571.
- [86] A. Yarlagadda, S. Kaushik, A.H. Clayton, Blood brain barrier: the role of calcium homeostasis, *Psychiatry* 4 (12) (2007) 55.
- [87] A. Lalatsa, A.M. Butt, Physiology of the Blood–Brain Barrier and Mechanisms of Transport across the BBB, *Nanotechnology-Based Targeted Drug Delivery Systems for Brain Tumors*, Elsevier, 2018, pp. 49–74.
- [88] S. Brady, *Basic Neurochemistry: Principles of Molecular, Cellular, and Medical Neurobiology*, Academic press, 2011.
- [89] A. Wong, M. Ye, A. Levy, J. Rothstein, D. Bergles, P.C. Searson, The blood–brain barrier: an engineering perspective, *Front. Neuroeng.* 6 (2013) 7.
- [90] W. Abdullahi, D. Tripathi, P.T. Ronaldson, Blood–brain barrier dysfunction in ischemic stroke: targeting tight junctions and transporters for vascular protection,

- Am. J. Physiol. Cell Physiol. 315 (3) (2018) C343–C356.
- [91] A. Montagne, Z. Zhao, B.V. Zlokovic, Alzheimer's disease: a matter of blood–brain barrier dysfunction? *J. Exp. Med.* 214 (11) (2017) 3151–3169.
- [92] M. Merlini, V.A. Rafalski, P.E.R. Coronado, T.M. Gill, M. Ellisman, G. Muthukumar, K.S. Subramanian, J.K. Ryu, C.A. Syme, D. Davalos, Fibrinogen induces microglia-mediated spine elimination and cognitive impairment in an Alzheimer's disease model, *Neuron* 101 (6) (2019) 1099–1108 e6.
- [93] M.A. Erickson, W.A. Banks, Blood–brain barrier dysfunction as a cause and consequence of Alzheimer's disease, *J. Cereb. Blood Flow Metab.* 33 (10) (2013) 1500–1513.
- [94] Z. Zhao, A.R. Nelson, C. Betsholtz, B.V. Zlokovic, Establishment and dysfunction of the blood–brain barrier, *Cell* 163 (5) (2015) 1064–1078.
- [95] N.J. Abbott, A.A. Patabendige, D.E. Dolman, S.R. Yusof, D.J. Begley, Structure and function of the blood–brain barrier, *Neurobiol. Dis.* 37 (1) (2010) 13–25.
- [96] P. Ballabh, A. Braun, M. Nedergaard, The blood–brain barrier: an overview: structure, regulation, and clinical implications, *Neurobiol. Dis.* 16 (1) (2004) 1–13.
- [97] M. Fisher, Pericyte signaling in the neurovascular unit, *Stroke* 40 (3 suppl 1) (2009) S13–S15.
- [98] A. Armulik, G. Genové, M. Mäe, M.H. Nisancioglu, E. Wallgard, C. Niaudet, L. He, J. Norlin, P. Lindblom, K. Strittmatter, Pericytes regulate the blood–brain barrier, *Nature* 468 (7323) (2010) 557.
- [99] A. ElAli, P. Thériault, S. Rivest, The role of pericytes in neurovascular unit remodeling in brain disorders, *Int. J. Mol. Sci.* 15 (4) (2014) 6453–6474.
- [100] C. Schrimpf, O.E. Teebken, M. Wilhelm, J.S. Duffield, The role of pericyte detachment in vascular rarefaction, *J. Vasc. Res.* 51 (4) (2014) 247–258.
- [101] J.R. Cirrito, R. Deane, A.M. Fagan, M.L. Spinner, M. Parsadanian, M.B. Finn, H. Jiang, J.L. Prior, A. Sagare, K.R. Bales, P-glycoprotein deficiency at the blood–brain barrier increases amyloid- β deposition in an Alzheimer disease mouse model, *J. Clin. Investig.* 115 (11) (2005) 3285–3290.
- [102] H. Girouard, C. Iadecola, Neurovascular coupling in the normal brain and in hypertension, stroke, and Alzheimer disease, *J. Appl. Physiol.* 100 (1) (2006) 328–335.
- [103] X. Jiang, A.V. Andjelkovic, L. Zhu, T. Yang, M.V. Bennett, J. Chen, R.F. Keep, Y. Shi, Blood–brain barrier dysfunction and recovery after ischemic stroke, *Prog. Neurobiol.* 163 (2018) 144–171.
- [104] D.B. Stanimirovic, J. Wong, A. Shapiro, J. Durkin, Increase in Surface Expression of ICAM-1, VCAM-1 and E-Selectin in Human Cerebrovascular Endothelial Cells Subjected to Ischemia-like Insults, *Brain Edema X*, Springer, 1997, pp. 12–16.
- [105] C. Frijns, L. Kappelle, Inflammatory cell adhesion molecules in ischemic cerebrovascular disease, *Stroke* 33 (8) (2002) 2115–2122.
- [106] P. Ballabh, A. Braun, M. Nedergaard, The blood–brain barrier: an overview: structure, regulation, and clinical implications, *Neurobiol. Dis.* 16 (1) (2004) 1–13.
- [107] W.C. Aird, Endothelial cell heterogeneity, *Crit. Care Med.* 31 (4 Suppl) (2003) S221–S30.
- [108] S. Nag, Morphology and properties of brain endothelial cells, *Methods Mol. Biol.* 686 (2011) 3–47.
- [109] F. Braet, E. Wisse, Structural and functional aspects of liver sinusoidal endothelial cell fenestrae: a review, *Comp. Hepatol.* 1 (1) (2002) 1.
- [110] E. Dejana, K.K. Hirschi, M. Simons, The molecular basis of endothelial cell plasticity, *Nat. Commun.* 8 (2017) 14361.
- [111] K.Y.Y. Fung, G.D. Fairn, W.L. Lee, Transcellular vesicular transport in epithelial and endothelial cells: challenges and opportunities, *Traffic* 19 (1) (2018) 5–18.
- [112] B.L. Coomber, P.A. Stewart, Morphometric analysis of CNS microvascular endothelium, *Microvasc. Res.* 30 (1) (1985) 99–115.
- [113] P.M. Gross, N.M. Sposito, S.E. Pettersen, J.D. Fenstermacher, Differences in function and structure of the capillary endothelium in gray matter, white matter and a circumventricular organ of rat brain, *Blood Vessel.* 23 (6) (1986) 261–270.
- [114] M. Simionescu, N. Simionescu, G.E. Palade, Morphometric data on the endothelium of blood capillaries, *J. Cell Biol.* 60 (1) (1974) 128–152.
- [115] W.P. Ge, W. Zhou, Q. Luo, L.Y. Jan, Y.N. Jan, Dividing glial cells maintain differentiated properties including complex morphology and functional synapses, *Proc. Natl. Acad. Sci. U.S.A.* 106 (1) (2009) 328–333.
- [116] M.V. Sofroniew, H.V. Vinters, Astrocytes: biology and pathology, *Acta Neuropathol.* 119 (1) (2010) 7–35.
- [117] A.F. McCaslin, B.R. Chen, A.J. Radosevich, B. Cauli, E.M. Hillman, *In vivo* 3D morphology of astrocyte–vasculature interactions in the somatosensory cortex: implications for neurovascular coupling, *J. Cereb. Blood Flow Metab.* 31 (3) (2011) 795–806.
- [118] Y. Zhang, B.A. Barres, Astrocyte heterogeneity: an underappreciated topic in neurobiology, *Curr. Opin. Neurobiol.* 20 (5) (2010) 588–594.
- [119] V. Matyash, H. Kettenmann, Heterogeneity in astrocyte morphology and physiology, *Brain Res. Rev.* 63 (1–2) (2010) 2–10.
- [120] M.A. Bylicky, G.P. Mueller, R.M. Day, Mechanisms of endogenous neuroprotective effects of astrocytes in brain injury, *Oxid. Med. Cell. Longev.* 2018 (2018) 6501031.
- [121] R. Cabezas, M. Ávila, J. Gonzalez, R.S. El-Bachá, E. Báez, L.M. García-Segura, J.C.J. Coronel, F. Capani, G.P. Cardona-Gomez, G.E. Barreto, Astrocytic modulation of blood brain barrier: perspectives on Parkinson's disease, *Front. Cell. Neurosci.* 8 (2014) 211.
- [122] N.J. Abbott, L. Rönnebeck, E. Hansson, Astrocyte–endothelial interactions at the blood–brain barrier, *Nat. Rev. Neurosci.* 7 (1) (2006) 41–53.
- [123] J.A. Hubbard, M.S. Hsu, M.M. Seldin, D.K. Binder, Expression of the astrocyte water channel aquaporin-4 in the mouse brain, *ASN Neuro* 7 (5) (2015) 1759091415605486.
- [124] H. Hibino, A. Fujita, K. Iwai, M. Yamada, Y. Kurachi, Differential assembly of inwardly rectifying K⁺ channel subunits, Kir4.1 and Kir5.1, in brain astrocytes, *J. Biol. Chem.* 279 (42) (2004) 44065–44073.
- [125] J. Satoh, H. Tabunoki, T. Yamamura, K. Arima, H. Konno, Human astrocytes express aquaporin-1 and aquaporin-4 *in vitro* and *in vivo*, *Neuropathology* 27 (3) (2007) 245–256.
- [126] R. Daneman, L. Zhou, A.A. Kebede, B.A. Barres, Pericytes are required for blood–brain barrier integrity during embryogenesis, *Nature* 468 (7323) (2010) 562–566.
- [127] R.C. Janzer, M.C. Raff, Astrocytes induce blood–brain barrier properties in endothelial cells, *Nature* 325 (6101) (1987) 253–257.
- [128] J.I. Alvarez, T. Katayama, A. Prat, Glial influence on the blood brain barrier, *Glia* 61 (12) (2013) 1939–1958.
- [129] N.J. Abbott, Astrocyte–endothelial interactions and blood–brain barrier permeability, *J. Anat.* 200 (6) (2002) 629–638.
- [130] D.M. Holtzman, J. Herz, G. Bu, Apolipoprotein E and apolipoprotein E receptors: normal biology and roles in Alzheimer disease, *Cold Spring Harb Perspect. Med.* 2 (3) (2012) a006312.
- [131] J.I. Alvarez, A. Dodelet-Devillers, H. Kebir, I. Ifergan, P.J. Fabre, S. Terouz, M. Sabbagh, K. Wosik, L. Bourbonniere, M. Bernard, J. van Horsen, H.E. de Vries, F. Charron, A. Prat, The Hedgehog pathway promotes blood–brain barrier integrity and CNS immune quiescence, *Science* 334 (6063) (2011) 1727–1731.
- [132] R.L. Stornetta, C.L. Hawelu-Johnson, P.G. Guyenet, K.R. Lynch, Astrocytes synthesize angiotensinogen in brain, *Science* 242 (4884) (1988) 1444–1446.
- [133] K. Wosik, R. Cayrol, A. Dodelet-Devillers, F. Berthelet, M. Bernard, R. Moudjian, A. Bouthillier, T.L. Reudelhuber, A. Prat, Angiotensin II controls occludin function and is required for blood–brain barrier maintenance: relevance to multiple sclerosis, *J. Neurosci.* 27 (34) (2007) 9032–9042.
- [134] N. Methia, P. André, A. Hafezi-Moghadam, M. Economopoulos, K.L. Thomas, D.D. Wagner, ApoE deficiency compromises the blood brain barrier especially after injury, *Mol. Med.* 7 (12) (2001) 810–815.
- [135] S.W. Lee, W.J. Kim, Y.K. Choi, H.S. Song, M.J. Son, I.H. Gelman, Y.J. Kim, K.W. Kim, SSeCKS regulates angiogenesis and tight junction formation in blood–brain barrier, *Nat. Med.* 9 (7) (2003) 900–906.
- [136] Y. Yao, Z.L. Chen, E.H. Norris, S. Strickland, Astrocytic laminin regulates pericyte differentiation and maintains blood brain barrier integrity, *Nat. Commun.* 5 (2014) 3413.
- [137] E. Colombo, C. Farina, Astrocytes: key regulators of neuroinflammation, *Trends Immunol.* 37 (9) (2016) 608–620.
- [138] D.J. Myer, G.G. Gurkoff, S.M. Lee, D.A. Hovda, M.V. Sofroniew, Essential protective roles of reactive astrocytes in traumatic brain injury, *Brain* 129 (Pt 10) (2006) 2761–2772.
- [139] M. Bélanger, P.J. Magistretti, The role of astroglia in neuroprotection, *Dialogues Clin. Neurosci.* 11 (3) (2009) 281–295.
- [140] C. Rouget, Mémoire sur le développement, la structure et les propriétés physiologiques des capillaires sanguins et lymphatiques, *Arch. Physiol. Norm.* 5 (1873) 603–663.
- [141] W. Roux, *Gesammelte Abhandlungen Über Entwicklungsmechanik der Organismen*, Wilhelm Engelmann, Leipzig, Germany, 1895.
- [142] W. Roux, *Theorie der Gestaltung der Blutgefäße Einschließlich des Kollateralkreislaufs*, Wilhelm Engelmann, Leipzig, 1910.
- [143] K.W. Zimmermann, Der feinere bau der blutcapillaren, *Z. Anat. Entwicklungsgesch.* 68 (1) (1923) 29–109.
- [144] M. Fisher, Pericyte signaling in the neurovascular unit, *Stroke* 40 (3 Suppl) (2009) S13–S5.
- [145] G. Bergers, S. Song, The role of pericytes in blood-vessel formation and maintenance, *Neuro Oncol.* 7 (4) (2005) 452–464.
- [146] A. Armulik, G. Genové, C. Betsholtz, Pericytes: developmental, physiological, and pathological perspectives, problems, and promises, *Dev. Cell* 21 (2) (2011) 193–215.
- [147] H. Zhao, J.C. Chappell, Microvascular bioengineering: a focus on pericytes, *J. Biol. Eng.* 13 (1) (2019) 26.
- [148] T. Dalkara, Y. Gursoy-Ozdemir, M. Yemisci, Brain microvascular pericytes in health and disease, *Acta Neuropathol.* 122 (1) (2011) 1–9.
- [149] J. Rustenhoven, D. Jansson, L.C. Smyth, M. Dragunow, Brain pericytes as mediators of neuroinflammation, *Trends Pharmacol. Sci.* 38 (3) (2017) 291–304.
- [150] C.N. Hall, C. Reynell, N.B. Hamilton, A. Mishra, B.A. Sutherland, F.M. O'Farrell, A.M. Buchan, M. Lauritzen, D. Attwell, Capillary pericytes regulate cerebral blood flow in health and disease, *Nature* 508 (7494) (2014) 55–60.
- [151] W.G. Chang, J.W. Andrejcsk, M.S. Kluger, W.M. Saltzman, J.S. Pober, Pericytes modulate endothelial sprouting, *Cardiovasc. Res.* 100 (3) (2013) 492–500.
- [152] J.T. Durham, H.K. Surks, B.M. Dulmovits, I.M. Herman, Pericyte contractility controls endothelial cell cycle progression and sprouting: insights into angiogenic switch mechanics, *Am. J. Physiol. Cell Physiol.* 307 (9) (2014) C878–C892.
- [153] G. Thanabalasundaram, J. Schneidewind, C. Pieper, H.-J. Galla, The impact of pericytes on the blood–brain barrier integrity depends critically on the pericyte differentiation stage, *Int. J. Biochem. Cell Biol.* 43 (9) (2011) 1284–1293.
- [154] B. Yue, Biology of the extracellular matrix: an overview, *J. Glaucoma* 23 (8 Suppl 1) (2014) S20–S3.
- [155] J.K. Kular, S. Basu, R.I. Sharma, The extracellular matrix: structure, composition, age-related differences, tools for analysis and applications for tissue engineering, *J. Tissue Eng.* 5 (2014) 2041731414557112.
- [156] D. Bonneh-Barkay, C.A. Wiley, Brain extracellular matrix in neurodegeneration, *Brain Pathol.* 19 (4) (2009) 573–585.
- [157] U. Novak, A.H. Kaye, Extracellular matrix and the brain: components and function, *J. Clin. Neurosci.* 7 (4) (2000) 280–290.

- [158] E.A. Turley, P.W. Noble, L.Y. Bourguignon, Signaling properties of hyaluronan receptors, *J. Biol. Chem.* 277 (7) (2002) 4589–4592.
- [159] G.D. Nicodemus, S.J. Bryant, Cell encapsulation in biodegradable hydrogels for tissue engineering applications, *Tissue Eng. Part B Rev* 14 (2) (2008) 149–165.
- [160] X. Xu, A.K. Jha, D.A. Harrington, M.C. Farach-Carson, X. Jia, Hyaluronic acid-based hydrogels: from a natural polysaccharide to complex networks, *Soft Matter* 8 (12) (2012) 3280–3294.
- [161] Y. Yamaguchi, Lecticans: organizers of the brain extracellular matrix, *Cell. Mol. Life Sci.* 57 (2) (2000) 276–289.
- [162] G. Klein, M. Langegger, R. Timpl, P. Ekblom, Role of laminin A chain in the development of epithelial cell polarity, *Cell* 55 (2) (1988) 331–341.
- [163] K.M. Yamada, Fibronectin and other cell interactive glycoproteins, in: E.D. Hay (Ed.), *Cell Biology of Extracellular Matrix*, Springer, Boston, MA, 1991, pp. 111–146.
- [164] K. Kühn, Basement membrane (type IV) collagen, *Matrix Biol.* 14 (6) (1995) 439–445.
- [165] T. Tilling, D. Korte, D. Hoheisel, H.J. Galla, Basement membrane proteins influence brain capillary endothelial barrier function *in vitro*, *J. Neurochem.* 71 (3) (1998) 1151–1157.
- [166] T. Tilling, C. Engelbertz, S. Decker, D. Korte, S. Hüwel, H.-J. Galla, Expression and adhesive properties of basement membrane proteins in cerebral capillary endothelial cell cultures, *Cell Tissue Res.* 310 (1) (2002) 19–29.
- [167] J.T. Morgan, J.A. Wood, N.M. Shah, M.L. Hughbanks, P. Russell, A.I. Barakat, C.J. Murphy, Integration of basal topographic cues and apical shear stress in vascular endothelial cells, *Biomaterials* 33 (16) (2012) 4126–4135.
- [168] M.S. Thomsen, L.J. Routhe, T. Moos, The vascular basement membrane in the healthy and pathological brain, *J. Cereb. Blood Flow Metab.* 37 (10) (2017) 3300–3317.
- [169] S.J. Liliensiek, J.A. Wood, J. Yong, R. Auerbach, P.F. Nealey, C.J. Murphy, Modulation of human vascular endothelial cell behaviors by nanotopographic cues, *Biomaterials* 31 (20) (2010) 5418–5426.
- [170] J.Z. Gasiorowski, S.J. Liliensiek, P. Russell, D.A. Stephan, P.F. Nealey, C.J. Murphy, Alterations in gene expression of human vascular endothelial cells associated with nanotopographic cues, *Biomaterials* 31 (34) (2010) 8882–8888.
- [171] S.J. Liliensiek, P. Nealey, C.J. Murphy, Characterization of endothelial basement membrane nanotopography in rhesus macaque as a guide for vessel tissue engineering, *Tissue Eng. A* 15 (9) (2009) 2643–2651.
- [172] L. Cucullo, M. Hossain, V. Puvenna, N. Marchi, D. Janigro, The role of shear stress in Blood-Brain Barrier endothelial physiology, *BMC Neurosci.* 12 (1) (2011) 40.
- [173] S. Jalali, M.A. del Pozo, K. Chen, H. Miao, Y. Li, M.A. Schwartz, J.Y. Shyy, S. Chien, Integrin-mediated mechanotransduction requires its dynamic interaction with specific extracellular matrix (ECM) ligands, *Proc. Natl. Acad. Sci. U.S.A.* 98 (3) (2001) 1042–1046.
- [174] E. Tzima, M.A. del Pozo, S.J. Shattil, S. Chien, M.A. Schwartz, Activation of integrins in endothelial cells by fluid shear stress mediates Rho-dependent cytoskeletal alignment, *EMBO J.* 20 (17) (2001) 4639–4647.
- [175] E.S. Lippmann, A. Al-Ahmad, S.M. Azarin, S.P. Palecek, E.V. Shusta, A retinoic acid-enhanced, multicellular human blood-brain barrier model derived from stem cell sources, *Sci. Rep.* 4 (2014) 4160.
- [176] A. Appelt-Menzel, A. Cubukova, K. Günther, F. Edenhofer, J. Piontek, G. Krause, T. Stüber, H. Walles, W. Neuhaus, M. Metzger, Establishment of a human blood-brain barrier co-culture model mimicking the neurovascular unit using induced pluripotent stem cells, *Stem Cell Rep* 8 (4) (2017) 894–906.
- [177] D. Qi, S. Wu, H. Lin, M.A. Kuss, Y. Lei, A. Krasnoslobodtsev, S. Ahmed, C. Zhang, H.J. Kim, P. Jiang, Establishment of a human iPSC-and nanofiber-based microphysiological blood-brain barrier system, *ACS Appl. Mater. Interfaces* 10 (26) (2018) 21825–21835.
- [178] H. Xu, Z. Li, Y. Yu, S. Sizdahkhani, W.S. Ho, F. Yin, L. Wang, G. Zhu, M. Zhang, L. Jiang, Z. Zhuang, J. Qin, A dynamic *in vivo*-like organotypic blood-brain barrier model to probe metastatic brain tumors, *Sci. Rep.* 6 (2016) 36670.
- [179] N.R. Wevers, D.G. Kasi, T. Gray, K.J. Wilschut, B. Smith, R. van Vught, F. Shimizu, Y. Sano, T. Kanda, G. Marsh, A perfused human blood-brain barrier on-a-chip for high-throughput assessment of barrier function and antibody transport, *Fluids Barriers CNS* 15 (1) (2018) 23.
- [180] S. Jeong, S. Kim, J. Buonocore, J. Park, C.J. Welsh, J. Li, A. Han, A Three-dimensional arrayed microfluidic blood-brain barrier model with integrated electrical sensor array, *IEEE Trans. Biomed. Eng.* 65 (2) (2018) 431–439.
- [181] R. Booth, H. Kim, Characterization of a microfluidic *in vitro* model of the blood-brain barrier (μ BBB), *Lab Chip* 12 (10) (2012) 1784–1792.
- [182] Y.I. Wang, H.E. Abaci, M.L. Shuler, Microfluidic blood-brain barrier model provides *in vivo*-like barrier properties for drug permeability screening, *Biotechnol. Bioeng.* 114 (1) (2017) 184–194.
- [183] J.D. Wang, E.-S. Khafagy, K. Khanafer, S. Takayama, M.E. ElSayed, Organization of endothelial cells, pericytes, and astrocytes into a 3d microfluidic *in vitro* model of the blood-brain barrier, *Mol. Pharm.* 13 (3) (2016) 895–906.
- [184] Y. Koo, B.T. Hawkins, Y. Yun, Three-dimensional (3D) tetra-culture brain on chip platform for organophosphate toxicity screening, *Sci. Rep.* 8 (1) (2018) 2841.
- [185] B.M. Maaz, A. Herland, E.A. FitzGerald, T. Grevesse, C. Vidoudez, A.R. Pacheco, S.P. Saezy, T.E. Park, S. Dauth, R. Mannix, N. Budnik, K. Shores, A. Cho, J.C. Nawroth, D. Segre, B. Budnik, D.E. Ingber, K.K. Parker, A linked organ-on-chip model of the human neurovascular unit reveals the metabolic coupling of endothelial and neuronal cells, *Nat. Biotechnol.* 36 (9) (2018) 865–874.
- [186] S.P. Deosarkar, B. Prabhakarandian, B. Wang, J.B. Sheffield, B. Krynska, M.F. Kiani, A novel dynamic neonatal blood-brain barrier on a chip, *PLoS One* 10 (11) (2015) e0142725.
- [187] E. Urich, C. Patsch, S. Aigner, M. Graf, R. Iacone, P.O. Freskgard, Multicellular self-assembled spheroidal model of the blood brain barrier, *Sci. Rep.* 3 (2013) 1500.
- [188] M.E. Boutin, L.L. Kramer, L.L. Livi, T. Brown, C. Moore, D. Hoffman-Kim, A three-dimensional neural spheroid model for capillary-like network formation, *J. Neurosci. Methods* 299 (2018) 55–63.
- [189] C.-F. Cho, J.M. Wolfe, C.M. Fadden, D. Calligaris, K. Hornburg, E.A. Chioocca, N.Y. Agar, B.L. Pentelute, S.E. Lawler, Blood-brain-barrier spheroids as an *in vitro* screening platform for brain-penetrating agents, *Nat. Commun.* 8 (2017) 15623.
- [190] G. Nzou, R.T. Wicks, E.E. Wicks, S.A. Seale, C.H. Sane, A. Chen, S.V. Murphy, J.D. Jackson, A.J. Atala, Human cortex spheroid with a functional blood brain barrier for high-throughput neurotoxicity screening and disease modeling, *Sci. Rep.* 8 (1) (2018) 7413.
- [191] M. Campisi, Y. Shin, T. Osaki, C. Hajal, V. Chiono, R.D. Kamm, 3D self-organized microvascular model of the human blood-brain barrier with endothelial cells, pericytes and astrocytes, *Biomaterials* 180 (2018) 117–129.
- [192] G. Adriani, D. Ma, A. Pavesi, R.D. Kamm, E.L. Goh, A 3D neurovascular microfluidic model consisting of neurons, astrocytes and cerebral endothelial cells as a blood-brain barrier, *Lab Chip* 17 (3) (2017) 448–459.
- [193] S. Bang, S.-R. Lee, J. Ko, K. Son, D. Tahk, J. Ahn, C. Im, N.L. Jeon, A low permeability microfluidic blood-brain barrier platform with direct contact between perfusable vascular network and astrocytes, *Sci. Rep.* 7 (1) (2017) 8083.
- [194] A. Herland, A.D. van der Meer, E.A. FitzGerald, T.E. Park, J.J. Sleetboom, D.E. Ingber, Distinct contributions of astrocytes and pericytes to neuroinflammation identified in a 3D human blood-brain barrier on a chip, *PLoS One* 11 (3) (2016) e0150360.
- [195] H. Uwamori, T. Higuchi, K. Arai, R. Sudo, Integration of neurogenesis and angiogenesis models for constructing a neurovascular tissue, *Sci. Rep.* 7 (1) (2017) 17349.
- [196] P.P. Partyka, G.A. Godsey, J.R. Galie, M.C. Kosciuk, N.K. Acharya, R.G. Nagele, P.A. Galie, Mechanical stress regulates transport in a compliant 3D model of the blood-brain barrier, *Biomaterials* 115 (2017) 30–39.
- [197] J.A. Brown, V. Pensabene, D.A. Markov, V. Allwardt, M.D. Neely, M. Shi, C.M. Britt, O.S. Hoilet, Q. Yang, B.M. Brewer, P.C. Samson, L.J. McCawley, J.M. May, D.J. Webb, D. Li, A.B. Bowman, R.S. Reiserer, J.P. Wiksw, Recreating blood-brain barrier physiology and structure on chip: a novel neurovascular microfluidic bioreactor, *Biomicrofluidics* 9 (5) (2015) 054124.
- [198] H. Cho, J.H. Seo, K.H. Wong, Y. Terasaki, J. Park, K. Bong, K. Arai, E.H. Lo, D. Irimia, Three-dimensional blood-brain barrier model for *in vitro* studies of neurovascular pathology, *Sci. Rep.* 5 (2015) 15222.
- [199] J.A. Kim, H.N. Kim, S.-K. Im, S. Chung, J.Y. Kang, N. Choi, Collagen-based brain microvasculature model *in vitro* using three-dimensional printed template, *Biomicrofluidics* 9 (2) (2015) 024115.
- [200] B. Srinivasan, A.R. Kolli, M.B. Esch, H.E. Abaci, M.L. Shuler, J.J. Hickman, TEER measurement techniques for *in vitro* barrier model systems, *J. Lab. Autom.* 20 (2) (2015) 107–126.
- [201] A. Thomas, S. Wang, S. Sohrabi, C. Orr, R. He, W. Shi, Y. Liu, Characterization of vascular permeability using a biomimetic microfluidic blood vessel model, *Biomicrofluidics* 11 (2) (2017) 024102.
- [202] A.M. Butt, H.C. Jones, N.J. Abbott, Electrical resistance across the blood-brain barrier in anaesthetized rats: a developmental study, *J. Physiol.* 429 (1) (1990) 47–62.
- [203] C. Crone, S. Olesen, Electrical resistance of brain microvascular endothelium, *Brain Res.* 241 (1) (1982) 49–55.
- [204] G.D. Vatine, R. Barrile, M.J. Workman, S. Sances, B.K. Barriga, M. Rahnama, S. Barthakur, M. Kasendra, C. Lucchesi, J. Kerns, Human iPSC-derived blood-brain barrier chips enable disease modeling and personalized medicine applications, *Cell stem cell* 24 (6) (2019) 995–1005 e6.
- [205] G.D. Vatine, A. Al-Ahmad, B.K. Barriga, S. Svendsen, A. Salim, L. Garcia, V.J. Garcia, R. Ho, N. Yucer, T. Qian, Modeling psychomotor retardation using iPSCs from MCT8-deficient patients indicates a prominent role for the blood-brain barrier, *Cell Stem Cell* 20 (6) (2017) 831–843 e5.
- [206] O. Chaudhuri, L. Gu, D. Klumpers, M. Darnell, S.A. Bencherif, J.C. Weaver, N. Huebsch, H.P. Lee, E. Lippens, G.N. Duda, D.J. Mooney, Hydrogels with tunable stress relaxation regulate stem cell fate and activity, *Nat. Mater.* 15 (3) (2016) 326–334.
- [207] A.J. Engler, S. Sen, H.L. Sweeney, D.E. Discher, Matrix elasticity directs stem cell lineage specification, *Cell* 126 (4) (2006) 677–689.
- [208] A. Sobrino, D.T. Phan, R. Datta, X. Wang, S.J. Hachey, M. Romero-Lopez, E. Grattan, A.P. Lee, S.C. George, C.C. Hughes, 3D microtumors *in vitro* supported by perfused vascular networks, *Sci. Rep.* 6 (2016) 31589.
- [209] V.W. van Hinsbergh, A. Collen, P. Koolwijk, Role of fibrin matrix in angiogenesis, *Ann. N. Y. Acad. Sci.* 936 (1) (2001) 426–437.
- [210] K.T. Morin, R.T. Tranquillo, *In vitro* models of angiogenesis and vasculogenesis in fibrin gel, *Exp. Cell Res.* 319 (16) (2013) 2409–2417.
- [211] A.C. Newman, M.N. Nakatsu, W. Chou, P.D. Gershon, C.C. Hughes, The requirement for fibroblasts in angiogenesis: fibroblast-derived matrix proteins are essential for endothelial cell lumen formation, *Mol. Biol. Cell* 22 (20) (2011) 3791–3800.
- [212] M.N. Nakatsu, R.C. Sainson, J.N. Aoto, K.L. Taylor, M. Aitkenhead, S. Perez-del-Pulgar, P.M. Carpenter, C.C. Hughes, Angiogenic sprouting and capillary lumen formation modeled by human umbilical vein endothelial cells (HUVEC) in fibrin gels: the role of fibroblasts and Angiopoietin-1, *Microvasc. Res.* 66 (2) (2003) 102–112.
- [213] S. Kim, H. Lee, M. Chung, N.L. Jeon, Engineering of functional, perfusable 3D microvascular networks on a chip, *Lab Chip* 13 (8) (2013) 1489–1500.
- [214] S. Kim, M. Chung, J. Ahn, S. Lee, N.L. Jeon, Interstitial flow regulates the angiogenic response and phenotype of endothelial cells in a 3D culture model, *Lab Chip*

- 16 (21) (2016) 4189–4199.
- [215] H. Duvernoy, S. Delon, J.L. Vannson, The vascularization of the human cerebellar cortex, *Brain Res. Bull.* 11 (4) (1983) 419–480.
- [216] K. Benson, S. Cramer, H.-J. Galla, Impedance-based cell monitoring: barrier properties and beyond, *Fluids Barriers CNS* 10 (1) (2013) 5.
- [217] L. Griep, F. Wolbers, B. De Wagenaar, P.M. ter Braak, B. Weksler, I.A. Romero, P. Couraud, I. Vermes, A.D. van der Meer, A. van den Berg, BBB on chip: microfluidic platform to mechanically and biochemically modulate blood-brain barrier function, *Biomed. Microdevices* 15 (1) (2013) 145–150.
- [218] J. Wegener, D. Abrams, W. Willenbrink, H.-J. Galla, A. Janshoff, Automated multi-well device to measure transepithelial electrical resistances under physiological conditions, *Biotechniques* 37 (4) (2004) 590–597.
- [219] J. Wegener, S. Zink, P. Rösen, H.-J. Galla, Use of electrochemical impedance measurements to monitor β -adrenergic stimulation of bovine aortic endothelial cells, *Pflüg. Arch.* 437 (6) (1999) 925–934.
- [220] N.J. Douville, Y.-C. Tung, R. Li, J.D. Wang, M.E. El-Sayed, S. Takayama, Fabrication of two-layered channel system with embedded electrodes to measure resistance across epithelial and endothelial barriers, *Anal. Chem.* 82 (6) (2010) 2505–2511.
- [221] P.A. Vogel, S.T. Halpin, R.S. Martin, D.M. Spence, Microfluidic transendothelial electrical resistance measurement device that enables blood flow and postgrowth experiments, *Anal. Chem.* 83 (11) (2011) 4296–4301.
- [222] B. Weksler, I.A. Romero, P.-O. Couraud, The hCMEC/D3 cell line as a model of the human blood brain barrier, *Fluids Barriers CNS* 10 (1) (2013) 16.
- [223] E.S. Lippmann, A. Al-Ahmad, S.P. Palecek, E.V. Shusta, Modeling the blood–brain barrier using stem cell sources, *Fluids Barriers CNS* 10 (1) (2013) 2.
- [224] A.C. da Fonseca, D. Matias, C. Garcia, R. Amaral, L.H. Geraldo, C. Freitas, F.R. Lima, The impact of microglial activation on blood-brain barrier in brain diseases, *Front. Cell. Neurosci.* 8 (2014) 362.
- [225] J.H. Seo, T. Maki, M. Maeda, N. Miyamoto, A.C. Liang, K. Hayakawa, L.D. Pham, F. Suwa, A. Taguchi, T. Matsuyama, M. Ihara, K.W. Kim, E.H. Lo, K. Arai, Oligodendrocyte precursor cells support blood-brain barrier integrity via TGF- β signaling, *PLoS One* 9 (7) (2014) e103174.
- [226] A.L. Placone, P.M. McGuiggan, D.E. Bergles, H. Guerrero-Cazares, A. Quinones-Hinojosa, P.C. Searson, Human astrocytes develop physiological morphology and remain quiescent in a novel 3D matrix, *Biomaterials* 42 (2015) 134–143.
- [227] M.W. van der Helm, M. Odijk, J.P. Frimat, A.D. van der Meer, J.C.T. Eijkel, A. van den Berg, L.I. Segerink, Direct quantification of transendothelial electrical resistance in organs-on-chips, *Biosens. Bioelectron.* 85 (2016) 924–929.